Inflammasome Profiling in Human Natural Killer Cells under Pro-inflammatory Stimuli and Solid Organ Transplantation

Antonio Astorga-Gamaza[1,2,*], Inés Muela-Zarzuela[1], Juan Miguel Suárez-Rivero[1], Alexis Varin[3], Maarten Naesens[4], Alessandra Tammaro[6], Jesper Kers[5,6,7], Juan López-Pérez[8,9], Raquel de la Varga-Martínez[8,9], Auxiliadora Mazuecos[9], Baptiste Lamarthée[3], and Mario D. Cordero[1,10, &]

[1] Department of Molecular Biology and Biochemical Engineering, Universidad Pablo de Olavide, 41013 Seville, Spain.

[2] Department of Medical Microbiology and Infection Prevention, Amsterdam University Medical Center (UMC), University of Amsterdam, Amsterdam, the Netherlands.

[3] Inserm UMR1098 Right, University Marie and Louis Pasteur, EFS BFC, Besançon, France.

[4] Department of Microbiology, Immunology and Transplantation, Nephrology and Kidney Transplantation Research Group, KU Leuven, Leuven, Belgium; Department of Nephrology and Kidney Transplantation, University Hospital Leuven, Leuven, Belgium.

[5] Department of Pathology, Amsterdam University Medical Center, Amsterdam, The Netherlands.

[6] Department of Pathology, Leiden University Medical Center, Leiden, The Netherlands

[7] Department of Pathology, Erasmus Medical Center, Rotterdam, The Netherlands

[8] Instituto de Investigación e Innovación Biomédica de Cádiz, INiBICA, Hospital Universitario Puerta del Mar, Cádiz, Spain.

[9] Department of Immunology, Puerta del Mar Hospital, 11009 Cádiz, Spain.

[10] CIBER de Enfermedades Respiratorias (CIBERES), Instituto de Salud Carlos III, 28220 Madrid, Spain.

[&]Corresponding author: Mario D. Cordero, PhD

Department of Molecular Biology and Biochemical Engineering, Universidad Pablo de Olavide, 41013 Seville, Spain. Email: mdcormor1@upo.es.

***Co-Corresponding author: Antonio Astorga Gamaza, PhD**

Department of Molecular Biology and Biochemical Engineering, Universidad Pablo de Olavide, 41013 Seville, Spain. Email: antonio.medina93@gmail.com.

Summary

Innate immunity relies on inflammasomes as key mediators of host defense, orchestrating the release of pro-inflammatory cytokines and triggering pyroptotic cell death in response to harmful stimuli. Although inflammasome activity has been extensively studied in myeloid cells, its role in natural killer (NK) cells remains underexplored. This study demonstrates that human primary NK cells can functionally activate inflammasomes both in vitro and in vivo, including in patients undergoing organ transplantation. Ex vivo stimulation with nigericin and the dipeptidyl peptidases (DPP) inhibitor Talabostat (Val-boroPro) induces pyroptotic cell death in a subset of NK cells. This is marked by the cleavage and activation of gasdermin D, a lytic pore-forming protein essential for pyroptosis. Accompanying gasdermin D activation, significant levels of lactate dehydrogenase (LDH) and residual amounts of interleukin-18 (IL-18) are released. The detection of activated caspase-4 further indicates that these processes are mediated through non-canonical inflammasome pathways in NK cells. Notably, $CD56^{dim}$ and $CD56^{bright}$ NK cell subsets exhibit distinct responses to pro-inflammatory stimulation. In patients with renal dysfunction, sustained inflammasome activation, particularly involving NLRP1 and NLRP3, is observed in NK cells, with a shift toward a more pro-inflammatory phenotype following kidney transplantation. Single-cell RNA sequencing analyses further reveal persistently elevated expression of caspase-4 and gasdermin-D in transplant recipients experiencing rejection and microvascular inflammation. These findings highlight the underappreciated role of NK cells in inflammasome-driven inflammation, underscoring their importance in both basic research and clinical contexts.

58 **Introduction**

59 Inflammation is part of the body's defense response to harmful stimuli. However,
60 exacerbated inflammation is also associated with a range of diseases. In this regard, the activity of
61 natural killer (NK) cells has been shown to highly depend on the context, helping to reduce or even
62 promote inflammatory processes [1].

63 NK cells are innate lymphoid cells characterized by a huge diversity of phenotypes and
64 functions [2, 3], although they are primarily categorized into two main subpopulations based on the
65 neural cell adhesion molecule CD56 density. $CD56^{dim}$ NK cells are known for their potent cytolytic
66 activities, and $CD56^{bright}$ NK cells are distinguished by their cytokine secretion capabilities [4]. They
67 play a pivotal role in immune surveillance, effectively targeting malignant and infected cells to
68 control intracellular pathogens and shaping adaptive immune responses [5]. Equipped with a huge
69 array of cell surface receptors, NK cells sense stress signals in target cells, distinguishing between
70 'self' and 'non-self' or 'aberrant' targets under normal physiological conditions [6]. Upon activation,
71 NK cells release cytotoxic granules containing perforin and granzyme. Also, they secrete interferon
72 (IFN)-γ and tumor necrosis factor (TNF), and immunoregulatory molecules such as interleukin (IL)-
73 10 and the growth factor GM-CSF, as well as chemokines including CCL3 (MIP-1α), CCL4 (MIP-1β),
74 CCL5 (RANTES), and CXCL8 (IL-8) [7]. Through these mechanisms, NK cells can drive inflammation
75 and modulate the activity of other immune cells.

76 A key part of the inflammatory process and the innate immune response is the assembly of
77 inflammasomes. These cytosolic multi-protein complexes regulate tissue inflammation in response
78 to multiple cellular stress patterns, including pathogen-associated molecular patterns (PAMPs) such
79 as bacterial lipopolysaccharide (LPS), or cellular damage-associated molecular patterns (DAMPs),
80 which include extracellular ATP and changes in intracellular ion concentrations. In this regard,
81 inflammasome biology has been mostly characterized in macrophages and at least partially studied
82 in other cell types such as endothelial cells, fibroblasts, epithelial cells, and T cells [8-11]. However,
83 it is unknown whether NK cells are equipped with functional inflammasome components, and thus,
84 this could represent an underexplored arm of the diverse immune mechanisms mediated by these
85 cells and an important source of inflammation.

86 The first steps in the triggering of inflammasomes comprise the detection of the damage
87 patterns via sensors of several families such as the NOD-like (NLR), Toll-like (TLR), AIM2-like (ALR),

88 or the caspase recruitment domain (CARD)-containing family of proteins, that include the members
89 NLRP1, NLRP3, NLRC4, AIM2, and CARD8, among others [12]. Following activation, some sensors
90 interact with adaptor proteins such as ASC (apoptosis-associated speck-like protein containing a
91 CARD), composing a pre-complex that then recruits inflammatory caspase-1. Next to terminal
92 assembly, the activation of caspase-1 in the inflammasome can lead to the proteolytic cleavage and
93 maturation of the IL-1 family cytokines IL-1β and IL-18 [13]. This pathway is known as the "canonical"
94 activation. Another usual key event after the inflammasome activation is the cleavage of
95 gasdermins, a family of pore-forming proteins, into its N-terminal active domain, which induces a
96 proinflammatory form of regulated cell death termed pyroptosis [14]. Inflammasome activation can
97 also occur in a named "non-canonical" way, with caspases-4 and -5 in humans directly promoting
98 pyroptosis [15, 16].

99 Herein, we conducted a transcriptomic analysis of NK cells derived from various tissues,
100 revealing the expression of genes encoding several components of the inflammasome. Additionally,
101 we provide proteomic evidence demonstrating the expression of all the components for the NLRP3
102 and NLRP1 inflammasome in both $CD56^{dim}$ and $CD56^{bright}$ NK cell subsets. More importantly, we
103 demonstrate the functionality of these inflammasomes in NK cells, mainly evidenced by the
104 induction of pyroptotic cell death and activation of gasdermin-D. Interestingly, we observe distinct
105 responses to pro-inflammatory stimuli between the two NK cell subpopulations. Furthermore, we
106 identify signs of inflammasome activation in NK cells from patients with renal dysfunction, which
107 persist despite immunosuppression after kidney transplantation. Our findings suggest that NK cells
108 should be considered in inflammation research and as potential therapeutic targets, as they might
109 play a role in both pathogen defense and inflammatory disorders through inflammasome signaling
110 and pyroptosis.

111 **RESULTS**

112 **Expression of inflammation-related genes in human NK cells from different tissues**

113 To gain insight into the potential of human NK cells in shaping inflammatory responses and
114 constituting functional inflammasomes, we conducted a transcriptomic analysis of NK cells from
115 diverse tissues using a publicly available RNA-seq dataset [3]. Cells were isolated from donors
116 without cancer or any other chronic disease, and seronegative for hepatitis B, C, and HIV viral
117 infections [3]. We assessed the expression of a list of genes related to inflammation, considering a
118 reference list [17]. From a total of 2,686 genes, we found expression of 1,619 in NK cells from blood,
119 bone marrow, lymph nodes, lungs, and spleen. These genes appeared to be involved in different
120 processes such as the regulation of the NF-κB activity, apoptosis, TNF signaling, cellular response to
121 lipopolysaccharide, NOD-like and Toll-like receptor signaling, IL-6 and IL-1β production (adjusted p
122 value < 0.05) (**Figure 1A**). Next, we performed a detailed analysis of the expression of short-listed
123 genes reported to play a role in activating inflammasome multiprotein complexes at different stages
124 (**Figure 1B, C, D, E, and F**). Interestingly, we noticed the expression in NK cells of guanylate-binding
125 proteins (GBP), which target intracellular pathogens and can mediate host defense via
126 inflammasome induction [18, 19]. Moreover, we found expression of other receptors of DAMPs and
127 PAMPs such as *TLR-2-3* and *4*, *NLRP1*, *NLRP3*, *NLRP6*, *NLRC3*, and *NLRC4,* the interferon-inducible
128 protein *AIM-2* and *CARD*. NK cells also expressed *PYCARD*, the gene coding for ASC protein, required
129 to constitute canonical inflammasomes, and the serin proteases *DPP8* and *DPP9*, whose
130 pharmacological inhibition by Val-boroPro (Vbp) (Talabostat) is reported to activate both NLRP1 and
131 CARD8 inflammasomes [20, 21]. Furthermore, NK cells from all analyzed tissues expressed
132 downstream effectors in the inflammasome pathway such as *CASPASE-1*, *IL-1β*, *IL-18*, and
133 *GASDERMIN D* genes (**Figure 1B, C, D, E, and F**). Some significant differences were noticed between
134 the NK subpopulations $CD56^{dim}$ and $CD56^{bright}$. This was the case for *GBP5* and *TLR3* in the blood
135 (**Figure 1B**), and *CASPASE-1* in the lung (**Figure 1C**), with higher expression in $CD56^{dim}$ NK cells.
136 However, larger datasets are needed to confirm and reveal differences between different NK
137 subpopulations as NK cells exhibit an intrinsic, highly heterogeneous nature intra- and inter-
138 individually [2].

139 Next, we aimed to assess the expression of the protein sensors NLRP1 and NLRP3, which have
140 been implicated in the regulation and pathogenesis of many conditions. We studied the expression
141 of the proteins NLRP1, NLRP3, and the adaptor ASC in NK cells by flow cytometry, using blood-

142 derived primary NK cells from healthy donors previously isolated by FACS (fluorescence-activated
143 cell sorting) (**Supplementary Figure 1A**). The median purity of the cells was 90.7% and 94.8% for
144 $CD56^{dim}$ and $CD56^{bright}$ NK cells, respectively. A representative example of staining can be found in
145 **Supplementary Figure 1B-C**. These proteins were widely expressed in circulating NK cells, with
146 slightly higher frequencies of ASC and NLRP1 in the $CD56^{bright}$ subpopulation (**Figure 1G and H**), but
147 no differences in the percentage of NLRP3 (**Figure 1I**) nor in the intensity of expression (mean
148 fluorescence intensity, MFI) of any of them (**Figure 1J, K, and L**). Our results indicate that both the
149 two main $CD56^{dim}$ and $CD56^{bright}$ subpopulations of NK cells express the components needed to
150 constitute functional inflammasomes, and particularly NLRP3 and NLRP1 inflammasomes,
151 suggesting that they may play a role in NK cell-mediated immunity.

152 **NK cell pyroptosis triggered by specific NLRP1 and NLRP3 inflammasome activators**

153 As a next step, we directly tested the functionality of inflammasomes in NK cells. For that, we
154 treated blood-derived NK cells from healthy volunteers, previously isolated by FACS, with
155 pharmacological activators of the NLRP3 and NLRP1 inflammasomes ex vivo. We included conditions
156 of cells cultured with lipopolysaccharide (LPS) plus ATP (LPS-ATP), nigericin (Nig), and the
157 DPP8/DPP9 inhibitor Vbp for both $CD56^{dim}$ and $CD56^{bright}$ NK subpopulations separately. Cytokine
158 secretion was barely detected, with minimal amounts of IL-18 upon stimulation of $CD56^{dim}$ cells with
159 nigericin (**Figure 2A**) or $CD56^{bright}$ cells with Vbp (**Figure 2B)**. No increment was detected in any of
160 the subpopulations after LPS-ATP stimulation (**Supplementary Figures 2A and B**). IL-1β was also not
161 induced *in vitro*, except for one donor that also showed higher levels of IL-6 (**Supplementary Figures**
162 **2C, D, and E**). Besides, we measured other immune mediators by a multiplex Luminex immunoassay.
163 The secretion of IL-10, GM-CSF, and the NK-associated cytotoxic and regulatory molecules IFN-γ,
164 IFN-α, or TNF-α was not detectable in our assay conditions, suggesting that in vitro treatment with
165 nigericin and Vbp does not induce unspecific NK cytotoxicity. Interestingly, ICAM-1, the adhesion
166 receptor and regulator of inflammation, seemed to increase its concentration after LPS-ATP and
167 nigericin treatment of $CD56^{dim}$ cells (**Supplementary Figures 2F and G**). These results suggest that
168 different pro-inflammatory stimuli might differentially affect distinct NK subpopulations.

169 Next, we assessed cell death by pyroptosis, a key process induced after inflammasome
170 activation. Notably, we detected the activation of the N-terminal fragment of gasdermin D (GSDMD-
171 Cleaved) by western blot after nigericin and Vbp treatment of NK cells (**Figure 2C**). Of note, this was
172 successfully detected only in $CD56^{dim}$ NK cells. However, the release of LDH, which confirms cell

173 death, was more prominent in the CD56^{bright} subpopulation (**Figure 2D and E**), raising the possibility
174 that more aggressive death of CD56^{bright} NK cells may hinder the detection of active gasdermin D.
175 Both pro-inflammatory cytokine secretion and gasdermin-dependent pyroptosis rely on the
176 previous cleavage of inflammatory caspases into their active form [13]. Here, we failed to observe
177 increased active fragments of caspase-1 in NK cells stimulated with nigericin and Vbp in 6 out of 7
178 experiments. Importantly, in additional experiments we aimed to measure activated caspase-4, and
179 it was successfully detected (**Figure 2F**), suggesting the non-canonical activation of the
180 inflammasomes in NK cells. Moreover, the inhibition of NLRP1 and NLRP3 using the dual inhibitor
181 ADS032 lowered the amount of activated caspase-4 in NK cells (**Figure 2F**).

182 **NLRP1 and NLRP3 undergo protein reorganization in NK cells under pro-inflammatory stimuli,**
183 **and their activation does not require ASC oligomerization**

184 To gain further insight into the activation of inflammasomes in NK cells, we assessed the
185 expression of proteins within control and treated cells. The purity of the cells employed in these
186 assays was always higher than 90.0%. Moreover, any remaining cell contaminants in the culture
187 were discarded from our analysis using lineage markers for NK cells in the flow cytometry panel.
188 Treatment of NK cells, CD56^{dim} or CD56^{bright}, with LPS-ATP, nigericin, or Vbp, did not alter the
189 frequency of cells expressing NLRP3 (**Figures 3A and B**), NLRP1 (**Figures 3C and D**), or ASC (**Figures**
190 **3E and F**). However, changes in the intensity of expression (MFI) were detected in the case of
191 nigericin exposure of CD56^{bright} NK cells, with a reduction in NLRP3 levels (**Figure 3G**). This was not
192 observed for the other proteins or stimuli (**Supplementary Figures 3A, B, C, D, and E**). This may
193 indicate that nigericin and Vbp promote the reorganization of these molecules to assemble the
194 inflammasomes rather than drastically changing their expression levels. Additionally, nigericin may
195 promote a more aggressive pyroptotic death of CD56^{bright} NK cells, which could explain the lower
196 levels of NLRP3 and higher LDH release (as shown in Figure 2D and E). Moreover, we studied the
197 formation of specks by flow cytometry, as previously reported [22]. In the formation of
198 inflammasomes, when canonical activation occurs, ASC interacts with upstream sensors such as
199 NLRP1 and NLRP3, which subsequently trigger its assembly into a structure known as a speck
200 composed of multimers of ASC dimers. The speck can be detected by flow cytometry using the time-
201 of-flight (TOF) signal of ASC, as it correlates with a higher pulse height-to-area (H:A) ratio (**Figure**
202 **3H)**. Despite consistent signs of speck in CD56^{dim} NK cells after nigericin stimulation, specking levels
203 were very low (**Figure 3I**). Treatment with Vbp also slightly induced specks in 5 out of 7 independent

204 assays in CD56^{bright} NK cells (**Figure 3J**). We did not detect any sign of speck in LPS-ATP or Vbp-treated
205 CD56^{dim} NK cells (**Supplementary Figures 3F and G**), nor consistently in LPS-ATP and nigericin treated
206 CD56^{bright} subpopulation (**Supplementary Figures 3H and I**). Next, we directly explored and
207 visualized the specking of ASC through fluorescent flow cytometry imaging (Amnis®). Primary
208 monocytes and NK cells treated with nigericin, with or without previous treatment with the NLRP1
209 and NLRP3 dual inhibitor ADS032, were acquired and gated based on the expression of CD3, CD56,
210 and CD14. As expected, we observed a fraction of monocytes with a cytosolic diffusion pattern of
211 ASC expression (**Figure 3K**), but also a significant fraction showing ASC assembly (**Figure 3L**), which
212 was lower in the presence of the dual inflammasome inhibitor ADS032 (**Figure 3M**). Unlike
213 monocytes, even though we still detected some NK cells with ASC specking (**Figures 3N and O**), ASC
214 assembly was rare in NK cells (**Figure 3P**), confirming the results of our flow cytometry assay.

215 Overall, our results indicate that activated gasdermin-D is inducible and functional in NK cells,
216 particularly by the NLRP3 and NLRP1 activators nigericin and Vbp. CD56^{dim} and CD56^{bright} NK cells
217 behave differently under pro-inflammatory stimulation. Of note, based on our mechanistic
218 exploration assays, we believe that the non-canonical pathway leads to the activation of
219 NLRP1/NLRP3 inflammasomes in NK cells. Alternatively, pyroptosis of NK cells activating these
220 inflammasomes may be hindering/underestimating the detection of the canonical pathway.

221 **NK cells display inflammasome activation in patients with kidney disease and undergoing**
222 **organ transplantation**

223 To elucidate if NK cells participate in the orchestration and maintenance of inflammatory
224 processes through inflammasome signaling *in vivo*, we studied this in the context of kidney disease
225 and organ transplantation. Recent data support the hypothesis that imbalanced inflammation might
226 be an important driver of kidney disease that may persist even after organ transplantation [23-27].
227 We collected PBMCs from patients with chronic kidney disease (**Supplementary Table 1**). Western
228 blotting studies showed high protein levels of NLRP1, active caspase-1, and gasdermin-D in the
229 blood of these patients before and during the first week after kidney transplantation (**Figure 4A and**
230 **Supplementary Figure 4**), confirming the activation of inflammasomes and pro-inflammatory cell
231 death by pyroptosis of circulating immune cells. We then specifically studied NK cells from these
232 PBMC. Importantly, flow cytometry analyses (as represented in **Supplementary Figures 5A and B**)
233 confirmed that nearly 100 % of NK cells in these patients expressed NLRP1 (**Figure 4B**), about 50 %
234 expressed ASC (**Figure 4C**), and a smaller fraction NLRP3, which increased three days after

235 transplantation (**Figure 4D**). We also detected a fraction of NK cells with signs of speck, which was
236 enriched three days post-transplantation (**Figure 4E and Supplementary Figure 5C**). Speck levels in
237 NK cells were much lower than those detected in monocytes, as expected (**Supplementary Figure**
238 **5D**). Additional analyses distinguishing between specking versus non-specking cells showed higher
239 levels of NLRP1 and NLRP3 in speck^{+} cells (**Figures 4F, G, H and I**), suggesting the activation of both
240 inflammasomes in NK cells from patients with renal dysfunction and shortly after undergoing organ
241 transplantation.

242 Microvascular inflammation (MVI) is a hallmark of immune-mediated injury of renal allografts,
243 characterized by immune cell infiltration into glomerular and peritubular capillaries. Traditionally,
244 MVI has been associated with antibody-mediated rejection (ABMR), but many MVI cases lack
245 detectable donor-specific antibodies (DSA), suggesting the involvement of other immune
246 mechanisms or alternative triggers such as ischemia/reperfusion and viral infections [28]. Recent
247 studies have emphasized the role of NK cells in this lesion [29-31]. To further dissect the molecular
248 expression patterns associated with the MVI observed in a fraction of kidney-transplanted
249 individuals, we conducted single-cell RNA-seq analyses of PBMC samples from a previous study on
250 kidney transplant recipients [32]. Clinical data of the patients are shown in **Supplementary Table 2**.
251 Several circulating immune cell clusters were analyzed (**Supplementary Figure 6A and B**). A pro-
252 inflammatory phenotype of NK cells in these individuals was confirmed, with more frequent
253 expression of *CASPASE-1*, *CASPASE-4*, *PYCARD/ASC*, *GASDERMIN-D*, *IL-18*, *GBP1*, *GBP5*, *STING*, and
254 *IFI16*, in both circulating CD56^{dim} and CD56^{bright} NK cells, compared to individuals lacking a
255 microvascular inflammatory signature in the biopsy (**Figure 4J**). This was detected despite a long
256 follow-up period after the transplant of up to 5.5 years for some of the patients participating in the
257 study. Notably, a significant increase in the intensity of expression of caspase-4 and gasdermin-D
258 was noticed in NK cells from patients with MVI, standing out over other immune cell subsets, and
259 confirming non-canonical inflammasome activation and pyroptosis in these cells, even after long
260 periods following transplantation (**Figure 4J**). Indeed, further classification of the data based on the
261 time after transplant in *mid-* (363-730 days) and *long-term* (+731 days) showed a peak of expression
262 of caspase-4 in NK cells at mid-term, approximately two years after receiving the organ
263 (**Supplementary Figure 7**).

264 Last, we investigated the transcriptional changes occurring in NK cells at the single-cell level in
265 kidney biopsies from transplanted patients with or without MVI, and the relationship with this

266 outcome. Single-cell RNA-seq publicly available datasets [30] of biopsies showing MVI or not were
267 selected as described in the Materials and Methods section. Structural compartments and several
268 immune cell clusters of the human transplanted kidney were analyzed (**Figure 5A and B**). scRNASeq
269 is not efficient to capture *NCAM1* expression encoding CD56, so we also used CD16 (*FCGR3A*) to
270 distingüish $CD56^{dim}$ and and $CD56^{bright}$ NK subpopulations. In addition, CD16 (*FCGR3A*+) NK cells
271 represent a subpopulation with potential to mediate antibody-dependent cell cytotoxicity (ADCC)
272 responses, highly relevant in the context of ABMR [31]. Clinical data from patients is summarized in
273 **Supplementary Table 3**. Similar to the results in peripheral blood, higher levels of caspase-4 were
274 found in CD16 (*FCGR3A*+)-expressing NK cells (**Figure 5C-D**), as well as higher NLRP1 and lower levels
275 of DPP8 and DPP9 in both $CD16^{+}$ and $CD16^{-}$ NK cells in biopsies with inflammatory lesions (**Figure**
276 **5C**). We did not observe an increase in gasdermin-D in renal NK cells, which could be attributed to
277 the cells undergoing pyroptosis more rapidly and thus dying. This inflammatory flux might promote
278 the migration of lymphocytes from circulation to inflamed kidneys and explain the higher
279 frequencies of immune effectors such as NK cells and T cells in biopsies showing MVI (**Figure 5E**).

280

281 **Discussion**

282 In this study, we shed light on the biology of inflammasomes in human NK cells, as dedicated
283 studies are lacking. These multiprotein complexes are involved in innate defense and inflammatory
284 responses to pathogens. Similarly, NK cells constitute a first line of defense against aberrant targets.
285 However, whether inflammasomes encompass one of their multiple immune mechanisms of action
286 and how it may impact health are unknown. Inflammasomes are composed of sensors, adaptors,
287 and effectors components, and their activation triggers the release of inflammatory cytokines and
288 pyroptosis [33]. Here, we show the expression of transcripts encoding several inflammasome-
289 forming proteins in NK cells distributed across different tissues. Sensors of several inflammasomes,
290 including the members of the NALP family NLRP3 and NLRP1 were found expressed. Consistent with
291 a prior report [34], we found a high constitutive expression of NLRP3. We also noticed high levels of
292 NLRP1 and the adaptor protein ASC in NK cells. More importantly, we prove here that
293 inflammasomes are functional in these cells and non-canonical activation can occur.

294 Several activators of the NLRP3 and NLRP1 inflammasomes have been identified, being reported
295 potassium ion (K^{+}) efflux as one of the most potent in the case of NLRP3 [35], and recently also

296 proven to activate NLRP1 [36], and inhibition of the serin dipeptidyl peptidases DPP8 and DPP9 for
297 NLRP1 activation [20, 21]. Here, we used Nigericin, a toxin derived from *Streptomyces hygroscopicus*
298 that facilitates H^+/K^+ anti-port across cell membranes and thereby causes potassium efflux [37], and
299 Vbp, an inhibitor of the inhibitory interaction between DPP8/DPP9 and NLRP1 [38], to assess the
300 functionality of both inflammasomes in NK cells. Our results revealed changes that are compatible
301 with inflammasome activation, including prominent signs of pyroptosis. Moreover, our experiments
302 seemed to indicate that the components of the NLRP3 and NLRP1 inflammasomes are more likely
303 to undergo a reorganization rather than upregulation upon stimulation with nigericin or Vbp.
304 Besides, we found differences in the response of $CD56^{dim}$ and $CD56^{bright}$ NK cells to both compounds.
305 This is not completely unexpected given the high plasticity and diversity in phenotypes and functions
306 of NK cells [2, 3]. Regarding the pore-forming protein gasdermin D, capable of inducing pyroptosis,
307 its active form was detected in $CD56^{dim}$ NK cells treated with nigericin and Vbp. LDH levels were also
308 increased in the culture of these cells, particularly in those treated with nigericin. Of note, although
309 we could not detect active gasdermin D in $CD56^{bright}$ cells, a notable release of LDH by these cells
310 was observed. The release of LDH is considered a surrogate of cell pyroptosis as large proteins are
311 usually filtered out in the absence of cell death [39]. Thus, it may be plausible that $CD56^{bright}$ NK cells
312 undergo more aggressive pyroptosis upon *in vitro* activation of the NLRP3/NLRP1 inflammasomes,
313 hindering the detection of active gasdermin-D. Also, the low numbers of these cells in the blood,
314 which usually represent less than 10% of circulating NK cells [40], may pose a technical challenge
315 for the detection of proteins. Alternatively, other forms of cell death could be involved. Different
316 frequencies and proportions of NK cell subpopulations can be found in tissues like the bone marrow,
317 spleen, lung, liver, lymph nodes, tonsils, and intestines [3]. Thus, further studies with different tissue
318 samples, NK subpopulations, and inflammasome-triggering agents or conditions could add valuable
319 insight into the biology of these lymphocytes and the inflammatory field.

320 To our knowledge, this is the first report clearly showing the inflammasome activation and
321 pyroptosis in human NK cells. Nevertheless, prior results in mice support our results, showing that
322 burn injury and radiation exposure induce the activation of caspase-1 in many cell subsets including
323 NK cells [41, 42]. Importantly, Fong et al also showed that the human pathogen group B
324 *Streptococcus* directly interacts with NK cells and suppresses a pyroptotic-like response via the
325 interaction with siglec-7 [43]. In this regard, our results did not show a typical inflammasome
326 response after the LPS-ATP stimulation of NK cells. However, this could be explained by the low
327 surface expression of TLR4 in these cells [44]. Thus, we do not rule out the possibility that direct

328 bacterial infection might activate some of the inflammasomes in NK cells. In fact, our transcriptomic
329 analysis showed that many other inflammasome sensors are transcriptionally expressed in these
330 cells, including NLRP6, NLRC4 or AIM-2, although if they are functional remain unknown and could
331 be more suitable after direct infections. Moreover, this evidence supports the notion that in vivo
332 different microenvironments and pathologic threads could trigger different inflammasome routes
333 in NK cells. Thus, the results presented here provide new insight into the biology of NK cells that
334 might support the role of these lymphocytes in different contexts via inflammasome activation.
335 Elucidating when these responses take place and whether they are beneficial or harmful could help
336 in the identification of new targets in inflammatory disorders.

337 Inflammasome activity has been associated with chronic kidney disease and kidney allograft
338 rejection, particularly linked to AIM-2, NLRP3, and more recently NLRP1 [23-27]. Here, we observed
339 signs of NLRP3 and NLRP1 inflammasome activation as well as activation of gasdermin-D in
340 circulating immune cells, including NK cells, in patients with end-stage kidney disease before and
341 after receiving a donor's kidney. Previously, it has been shown that post-transplantation NK cells
342 subsets can change even at the peripheral level, with variations in number and phenotype, and that
343 they are enriched in biopsies from patients with antibody-mediated rejection (ABMR) and
344 associated with inflammatory lesions in the microvascular compartment [30, 45].

345 Herein, we show the acquisition of a proinflammatory phenotype in NK cells shortly post-
346 transplantation, characterized by higher levels of NLRP1, NLRP3, and ASC, which persist long-term
347 marked by upregulated caspase-4. This suggests that different inflammatory milieus in vivo could
348 induce the activity of inflammasomes not only in classically studied subsets such as monocytes and
349 macrophages but also in innate lymphoid cells such as NK cells. Until now, two mechanisms have
350 been considered the main drivers for graft rejection in transplanted patients, T-cell-mediated
351 rejection, and/or antibody-mediated rejection. In both, NK cells have been shown to cooperate,
352 through the maturation of dendritic cells, activation of T cells, the triggering of missing-self
353 activation due to mismatches in HLA class I loci and NK inhibitory killer immunoglobulin-like
354 receptors (KIR), and mediating a pathogenic ADCC response triggered by anti-HLA antibodies in
355 $CD56^{dim}$ CD16-expressing NK cells [46]. Our results add evidence that NK cells might also contribute
356 to pathogenic inflammation in renal injured patients through pro-inflammatory activity via
357 inflammasome signaling. Although larger studies and longer follow-up periods are needed, our

358 results are tempting to speculate that inflammasome is a pathway by which NK cells might influence
359 renal disease and graft outcomes.

360 Recent studies have associated the activity of NK cells, particularly by Fc-receptor mediated
361 activation and ADCC, with graft injury patterns and ABMR, the principal process associated with MVI
362 [29-31, 47, 48]. This scenario requires the production of DSA able to mediate ADCC. Nevertheless,
363 many MVI cases lack detectable DSA [49, 50], suggesting the existence of multiple and alternative
364 immune mechanisms responsable for this inflammation. Both, DSA-positive (ABMR) and DSA-
365 negative MVI have been associated with similar NK cell burden [51], so they might be impacted by
366 similar NK cell activation mechanisms [28]. Some mechanisms have been proposed, including the
367 "missing-self" activation of NK cells, the IFN-γ response, and a particular receptor repertoir
368 potentially driving strong immune responses, although they do not fully explain the diverse and
369 complex nature of MVI [28]. Given the multifaceted role NK cells could play in MVI, targeting these
370 cells and their effector mechanisms could help reduce MVI. Indeed, in a recent phase 2 trial
371 conducted in late HLA DSA-positive ABMR patients, the anti-CD38 antibody "felzartamab", showed
372 promising results, substantially reducing MVI scores and with most patients converting to "no
373 ABMR" or an "inactive" ABMR phenotype [52]. Interestingly, this effect was accompanied by marked
374 decreases in the number of circulating NK cells and particular NK cell transcript sets [53]. Based on
375 our results, it could be hypothesized that NK cells are also relevant immune sensing effectors and
376 orchestrators of a pro-inflammatory response through inflammasome activation, potentially
377 recruiting other cell subsets such as monocytes/macrophages, neutrophils and T cells to the site of
378 inflammation, and thus sustaining this response. In this case, targeting inflammasomes and
379 preventing pyroptosis could represent an effective mechanism to reduce MVI. In this sense, several
380 inhibitors of gasdermin-D are being tested [54]. Moreover, in light of our results, both NLRP1 and
381 NLRP3 inflammasomes could be active and associated with MVI. Unfortunately, up to date, only one
382 dual-action molecule inhibitor targeting both the NLRP1 and NLRP3 inflammasomes has been
383 reported but it has not been clinically approved yet [55]. Thus, the development of dual
384 inflammasome-targeting pharmacological approaches could be highly beneficial in the context of
385 MVI and organ rejection.

386 Finally, we would light to emphasize that NK cells might play a role in several other inflammatory
387 diseases such as ischemic stroke, sepsis, or cancer, where persistent inflammasome activity and
388 activation of gasdermin D have been observed to cause undesired effects including organelle

389 dysfunction, cell lysis, and persistent release of cytokines [14]. Also, it will be relevant to determine
390 other contexts where inducing inflammasome activity of NK cells could be beneficial.

391 In conclusion, our findings underscore the importance of including NK cells in future studies
392 investigating inflammasome functionality in different clinical contexts.

393 **Acknowledgments**

394 M.D.C is supported by PI21/01656 grant from Instituto de Salud Carlos III, Spain, EMC21_00033 EMERGIA
395 program from Junta de Andalucia, AthenaDAO, PRF 2021-78 from Progeria Research Foundation, and
396 grant CNS2024-154939 from the Ministerio de Ciencia, Innovación y Universidades, Agencia Estatal de
397 Investigación. A.A.G was supported by the Spanish Secretariat of Science and Innovation post-doctoral
398 contract Juan de la Cierva (FJC2021-047304-I). The funders had no role in study design, data collection
399 and analysis, the decision to publish, or the preparation of the manuscript.

400 **Author contributions**

401 Conceptualization: A.A.G, M.D.C; Methodology: A.A.G, I.M.Z, AV, BL; Investigation: A.A.G, JM.S.R,
402 AT, JK, M.D.C; Resources: A.A.G, J.L.P, R.V.M, MN, AM, M.D.C; Visualization: A.A.G, I.M.Z, AV, AT, JK,
403 BL, M.D.C; Supervision: A.A.G, M.D.C; Funding acquisition: M.D.C; Writing – Original Draft: A.A.G;
404 Writing –Review & Editing: A.A.G, M.D.C.

405 **DECLARATION OF INTEREST**

406 The authors declare no competing interest.

407 **FIGURE LEGENDS**

408 **Figure 1. RNA-Seq analysis of inflammatory transcriptional signatures in circulating and tissue-**
409 **resident human NK cells, and protein expression of the NLRP1 and NLRP3 inflammasome sensors.**
410 Cells were isolated from donors without cancer or any other chronic disease, and seronegative for
411 hepatitis B, C, and HIV viral infections. **A)** Significance of the most represented immune pathways
412 according to the expression of a list of 2,686 inflammation-related genes. Functional gene
413 annotation was performed using DAVID. **B)** Heatmap of the expression of short-listed genes key in
414 the activation and triggering of effector functions of inflammasomes in circulating NK cells. An
415 analysis of the differential expression of these genes between $CD56^{bright}CD16^{-}$ and $CD56^{dim}CD16^{+}$ NK
416 cell subsets is also shown, and genes showing a different expression pattern between both NK
417 subpopulations are marked with a red box. The same is shown for **C)** NK cells in the lung, **D)** NK cells
418 in the lymph nodes, **E)** NK cells in the bone marrow, and **F)** NK cells in the spleen. Differentially
419 expressed genes were identified using linear models (Limma-Voom) and P values adjusted for

420 multiple comparisons by applying the Benjamini-Hochberg correction. **G)** Frequency (%) of
421 expression of ASC in sorted $CD56^{dim}CD16^{+}$ and $CD56^{bright}CD16^{-/dim}$ NK cells (n=8), **H)** Frequency of
422 NLRP1, and **I)** Frequency of NLRP3. Mean Fluorescence Intensity (MFI) signal for each marker in **J)**,
423 **K),** and **L)**. Median with range is represented. Statistical comparisons were performed using the
424 Wilcoxon matched-pairs signed-rank test.

425 **Figure 2**. **Activation of the NLRP1 and NLRP3 inflammasomes and induction of pyroptosis in human**
426 **NK cells ex vivo.** Isolated NK cells from blood samples were cultured in the presence of the
427 inflammasome activators LPS (1 µg/ml for 4 hours) and ATP (5 mM for 30 mins), nigericin (10 µM
428 for 30 mins) or Vbp (1 µM for 4 hours). After that, the concentration of cytokines of the IL-1 family
429 IL-18 and IL1β as well as lactate dehydrogenase (LDH) release were measured in the culture
430 supernatants. Changes in the cell expression of downstream effectors in the inflammasome cascade
431 such as caspase-1, caspase-4, and gasdermin D were also measured by western blot. **A)**
432 Concentration of IL-18 in cell cultures of untreated $CD56^{dim}$ NK cells or treated with nigericin (n=6).
433 **B)** IL-18 concentration in cell cultures of $CD56^{bright}$ NK cells stimulated with Vbp (n=5). **C)** Western
434 blot analysis of the full length and cleaved form of gasdermin D in $CD56^{dim}$ NK cells in basal
435 conditions and after nigericin and Vbp exposure. Representative result from n=5 independent
436 experiments. **D)** LDH release in cell cultures of stimulated $CD56^{dim}$ NK cells (n=6), and **E)** stimulated
437 $CD56^{bright}$ NK cells (n=6). **F)** Western blot analysis of the active forms of caspase-1 and caspase-4 in
438 NK cells after nigericin exposure and previous treatment with the NLRP1/NLRP3 inflammasome
439 inhibitor ADS032 before the nigericin stimulation.

440 **Figure 3**. **NLRP1, NLRP3, and adaptor ASC inflammasome protein levels in NK cells under different**
441 **proinflammatory stimuli**. **A)** to **G)** represent the frequency and MFI signal for the expression of
442 NLRP1, NLRP3 and ASC in $CD56^{dim}$ and $CD56^{bright}$ NK cells in non-stimulated and under pro-
443 inflammatory stimuli with LPS-ATP, nigericin, and Vbp conditions (n=8), measured by flow
444 cytometry. Graphs represent median with range. Statistical comparisons were performed using the
445 Wilcoxon matched-pairs signed-rank test. **H)** Representative flow cytometry plots of the time-of-
446 flight signal for ASC in NK cells, showing an increase in ASC area: height pulse, indicative of specking,
447 after nigericin in vitro stimulation. **I)** Graph showing the frequency of $CD56^{dim}$ NK cells with signs of
448 ASC specking after nigericin stimulation. **J)** The same for $CD56^{bright}$ NK cells stimulated with Vbp.
449 Statistical comparisons were performed using the Wilcoxon matched-pairs signed-rank test. **K)** and
450 **L)** Representative images of ASC expression in nigericin-stimulated monocytes $CD14^{+}$ obtained by
451 fluorescent imaging flow cytometry. Both patterns can be observed, diffuse ASC expression (**K**) and
452 speck structures (**L**). **M)** Frequency of monocytes with signs of ASC specking in nigericin-stimulated
453 cells with or without previous treatment with the dual NLRP1/NLRP3 inhibitor ADS032. The same
454 for NK cells ($CD56^{+}$) in **N)**, **O)** and **P)**.

455 **Figure 4**. **Inflammasome activation in NK cells from patients with chronic kidney disease and organ**
456 **transplantation.** Cells from peripheral blood samples of patients with renal disease collected at
457 different time points before and after kidney transplantation were studied. Activation of the
458 inflammasomes in these patients was investigated using western blotting, flow cytometry, and
459 single-cell RNA sequencing. **A)** Western blot representative results in total peripheral blood

460 mononuclear cells (PBMCs) from one renal-injured patient (#FJP in **Supplementary Table 1**),
461 showing the expression of NLRP1, NLRP3, pro-active caspase-1, the active fragment of caspase-1,
462 full-length gasdermin D, active gasdermin D, and the control β-actin, pre-transplantation and 3 and
463 7 days after being transplanted. **B)** Frequency of expression of NLRP1 in total $CD56^+$ NK cells (n=7).
464 **C)** Frequency of ASC. **D)** Frequency of NLRP3. **E)** Percentage of ASC specking in NK cells. Graphs
465 represent median with range. Statistical comparisons were performed using the Wilcoxon matched-
466 pairs signed-rank test. Graphs in **F)** and **G)** show the percentage and MFI of NLRP1 within $speck^-$ and
467 $speck^+$ NK cells at different time points. The same for NLRP3 in **H)** and **I).** Graphs represent median
468 with range. P values shown in the graphs represent ANOVA Friedman test, and asterisks denote the
469 multiple comparisons Dunn's test. *p<0.05; **p<0.01. Moreover, comparisons between the $speck^-$
470 and $speck^+$ NK cells at the same time points were performed using the Wilcoxon matched-pairs
471 signed-rank test. **J)** Single-cell RNA-sequencing (scRNAseq) analysis on 12 peripheral blood samples,
472 n=6 samples from kidney transplant recipients with a diagnosis of microvascular inflammation
473 (MVI), and n=6 patients without MVI. We show the expression of genes implicated in the
474 inflammasome pathways across the peripheral blood cells. cDC, conventional dendritic cell; ILC2,
475 innate lymphoid cell; NK, natural killer cell; NKT, natural killer T cell; PBMC, peripheral blood
476 mononuclear cell; pDC, plasmacytoid dendritic cell.

477 **Figure 5**. **A)** Analysis of scRNAseq data from kidney allograft biopsies (*n* =9 biopsies from 4 transplant
478 recipients with a diagnosis of microvascular inflammation (MVI), and 5 patients without MVI
479 (normal). Uniform Manifold Approximation and Projection (UMAP) plot of 20,607 cells passing QC
480 filtering. The main kidney cell types are represented, including loop of Henle (LOH), podocytes,
481 vascular smooth muscle and pericytes (vSMp), proximal tubule (PT), intercalated cells (IC), three
482 endothelial cell subsets comprising vasa recta (ECvr), glomerular (ECg) and peritubular capillaries
483 (ECptc), myeloid cells, and lymphoid cells such as FCGR3+ and FCGR3- NK cells. **B)** Dot plot showing
484 average gene expression values of canonical lineage markers (log scale) and percentage of major
485 cell types represented in the dataset and UMAP plot. **C)** Graph showing the expression of genes
486 implicated in the inflammasome pathways across the different cell types analyzed and comparing
487 between "normal" biopsies and those showing microvascular inflammation (MVI). **D)** Caspase-4
488 expression in *FCGR3*+ NK cells according to time after transplantation in kidney biopsies (Early: 0-31
489 days; Mid: 32-365 days; Late: >366 days). **E)** Relative proportions of the different cell types identified
490 in the kidney transplant biopsies.

491 **Supplementary Figure 1. A)** Example of the gating strategy for the identification of NK cells. **B)**
492 Example of the purity of the $CD56^{dim}$ and $CD56^{bright}$ NK cells after cell sorting. **C)** Flow-cytometry plots
493 showing a representative example for the expression of NLRP1, NLRP3, and ASC in $CD56^{dim}$ and
494 $CD56^{bright}$ NK cells, and the corresponding Fluorescence Minus One (FMO) control for the proper
495 gating.

496 **Supplementary Figure 2. A)** Concentration of IL-18 after the stimulation of $CD56^{dim}$ NK cells with
497 LPS-ATP. **B)** The same for $CD56^{bright}$ NK cells. **C)** Concentration of IL-1β after stimulation of $CD56^{dim}$
498 NK cells with nigericin, or **D)** with Vbp. **E)** Concentration of IL-6 in cell cultures of $CD56^{dim}$ NK cells
499 stimulated with Vbp, and **F)** concentration of ICAM-1 after LPS-ATP or **G)** nigericin stimulus.

500 **Supplementary Figure 3. A)** to **E)** Mean Fluorescence Intensity (MFI) signal for NLRP1, NLRP3 and
501 ASC in separate cultures of CD56^{dim} and CD56^{bright} NK cells basally and after pro-inflammatory
502 stimulation with LPS-ATP, nigericin or Vbp. Graphs represent median with range. **F)** to **I)** Frequency
503 (%) of specking cells within CD56^{dim} or CD56^{bright} NK cells after stimulation with LPS-ATP, nigericin or
504 Vbp. Statistical comparisons were performed using the Wilcoxon matched-pairs signed-rank test.

505 **Supplementary Figure 4.** Results from the analysis by western blot of the expression of several
506 inflammasome proteins in PBMCs from two patients with renal dysfunction (#MCB and #MFS in
507 **Supplementary Table 1**). This figure shows the expression of NLRP1, NLRP3, pro-active caspase-1,
508 the active fragment of caspase-1, full-length gasdermin D, active gasdermin D, and the control β-
509 actin, pre-transplantation and 3- and 7-days post-transplant.

510 **Supplementary Figure 5. A)** Representative example of the gating strategy used for the
511 identification of monocytes and NK cells in samples from patients with kidney dysfunction. **B)**
512 Representative plots of the expression of ASC, NLRP1 and NLRP3 in NK cells from these patients.
513 FMO controls are shown. **C)** Representative plot of the specking levels within NK cells from renal-
514 injured patients by the time-of-flight signal for ASC, showing an increase in ASC area: height pulse.
515 **D)** Frequency of speck^{+} monocytes in the samples from patients with renal dysfunction pre- and
516 post-transplant (n=7). The graph represents median with range and statistical comparisons were
517 performed using the Wilcoxon matched-pairs signed-rank test.

518 **Supplementary Figure 6.** Single-cell RNA-sequencing (scRNAseq) analysis on 12 peripheral blood
519 samples, n=6 samples from kidney transplant recipients with MVI, and n=6 patients without MVI. **A)**
520 Uniform Manifold Approximation and Projection (UMAP) representing several circulating immune
521 cell types, including lymphoid and myeloid cells. **B)** Dot plot showing average gene expression values
522 of canonical lineage markers (log scale) and percentage of major cell types represented in the
523 dataset (Figure 4J) and UMAP plot.

524 **Supplementary Figure 7.** Caspase-4 expression in **A)** CD56^{bright}CD16^{low} NK cells and **B)**
525 CD56^{dim}CD16^{bright} NK cells, according to time after transplantation in the different samples (*Mid*: 363-
526 730 days; *Late*: >731 days).

527 **Supplementary Table 1**. Clinical data of patients with renal dysfunction included in the study, and
528 sex and age of the organ donors.

529 **Supplementary Table 2**. Clinical data of patients included in the single cell transcriptomic analysis
530 of peripheral blood samples from kidney transplant recipients, comparing clinical parameters
531 between those with signs of MVI and those lacking MVI signature.

532 **Supplementary Table 3**. Clinical data of patients included in the scRNAseq analysis from kidney
533 allograft biopsies.

534 **MATERIALS AND METHODS**

535 <u>Human Samples</u>

536 In this study, we used primary cells obtained from blood samples from healthy donors or patients
537 with kidney disease and undergoing transplantation. Peripheral blood mononuclear cells (PBMCs)
538 were obtained from the Hospital Puerta del Mar in Cádiz, Spain. Study protocols were approved by
539 the corresponding Ethical Committees of the Hospital. All subjects recruited for this study were
540 adults who provided written informed consent. Information on renal disease parameters from
541 affected patients is summarized in Supplementary Table 1. Gender and age are also indicated in
542 Table S1 unless not available. Since we utilized samples from donors of different genders in our
543 experiments, we can conclude that the results reported here apply to both men and women. PBMCs
544 were obtained by Ficoll-Paque density gradient centrifugation. PBMCs were cultured in RPMI
545 medium (Gibco) supplemented with 10% Fetal Bovine Serum (Gibco), 1% streptomycin-penicillin
546 (Thermo Fisher, Waltham, MA, USA, 11548876) (R10 medium), and maintained at 37ºC in a 5% CO_2
547 incubator, when needed. NK cells were isolated from PBMCs by FACS (fluorescence-activated cell
548 sorting) (MELODY sorter) or using a commercial kit (MagniSort™ Human NK cell Enrichment;
549 eBioscience). The purity of the cells was always higher than 90%.

550 Transcriptomic analysis of a publicly available RNAseq data

551 We analyzed publicly available RNA-seq datasets. Data are available from Gene Expression
552 Omnibus (GEO) corresponding to the study with accession number GSE133383. This study provides
553 valuable transcriptomic data of two subpopulations of NK cells, $CD56^{dim}$ and $CD56^{bright}$, in tissues
554 difficult to obtain [3]. R version 4.1.2 was used to perform all bioinformatic analyses. Count values
555 were imported and processed using edgeR
556 [https://academic.oup.com/bioinformatics/article/26/1/139/182458?login=false]. Expression
557 values were normalized using the trimmed mean of M values (TMM) method and lowly-expressed
558 genes (<1 counts per million) were filtered out. Differentially expressed genes were identified using
559 linear models (Limma-Voom) [https://academic.oup.com/nar/article/43/7/e47/2414268], and P
560 values adjusted for multiple comparisons by applying the Benjamini-Hochberg correction. Heatmaps
561 were generated using the heatmap3 package [https://github.com/slzhao/heatmap3]. Glimma
562 [https://github.com/Shians/Glimma] was used for interactive visualizations. Functional gene
563 annotation was performed using DAVID [https://david.ncifcrf.gov].

564 Single-cell transcriptomic data analysis

565 Publicly available datasets corresponding to kidney allograft biopsies showing MVI or not were
566 selected from E-MTAB-12051 [30] as followed: EXT217 = Normal, EXT230 = MVI, EXT240 = MVI,

567 EXT241 = MVI, NEPH006 = Normal, NEPH011 = Normal, NEPH012 = Normal, NEPH014 = Normal,
568 NEPH015 = MVI. Publicly available datasets corresponding to PBMCs from kidney transplant
569 recipients showing MVI or not at the time of blood sample (Supplementary Table 2) were gathered
570 from E-MTAB-11450 [32]. Analysis was performed as previously described [30, 32], notably for
571 UMAP, grey scale dot plots and proportions. Viridis colored clustered dot plots were generated using
572 the DotPlot_Heatmap function from the R package RightOmicsTools: Varin, A.: An R Package
573 Providing Complementary Tools for the Manipulation and Visualization of Single Cell RNA-Seq Data.
574 Preprint at https://doi.org/10.5281/zenodo.12518909 (2025).
575

576 Human NK cell isolation by FACS

577 For Fluorescence Activated Cell Sorting (FACS), 80 million PBMCs were stained with LIVE/DEAD
578 AQUA viability (Invitrogen) for 20 minutes at RT. After washing with staining buffer (PBS 3% FBS),
579 cells were surface stained with anti-CD56-FITC (B159, Becton Dickinson), anti-CD3-PE-Cy7 (SK7,
580 Becton Dickinson), anti-CD16-BV786 (3G8, Becton Dickinson) and anti-CD4-APC (RPA-T4, Becton
581 Dickinson) antibodies for 20 minutes at RT. Cells were then washed with staining buffer and
582 immediately sorted using the MELODY Cell Sorter. We sorted the live populations $CD4^{-}CD3^{-}CD56^{dim}$
583 ($CD56^{dim}$ NK cells) and $CD4^{-}CD3^{-}CD56^{bright}$ ($CD56^{bright}$ NK cells). The purity of the cells was >90% in all
584 cases.

585 In vitro inflammasome activation assays

586 For in vitro pro-inflammatory stimulation, NK cells were treated with 1µg/ml LPS (Sigma-Aldrich, St.
587 Louis, MI, USA, L4391-1MG) for 4 hours and 5 mM ATP (Santa Cruz Biotechnology, Santa Cruz, CA,
588 USA, sc-214507A) for 30 mins. NK cells were also stimulated with 1 µM Val-boroPro (Sigma-Aldrich,
589 St. Louis, MI, USA, 5314650001) for 4 hours or 10 µM nigericin for 45 mins. As the number of isolated
590 NK cells varied between donors, we maintained the conditions of the cell culture, stimulating the
591 cells at a concentration of approximately 0,1M/ml, in 24-well plates for the $CD56^{dim}$ subpopulation
592 and 96-well plates for the $CD56^{bright}$ subpopulation. After the incubation, we collected culture
593 supernatants for LDH and cytokine measures, and cells for proteomics analyses by flow cytometry
594 or western blot. Controls consisting of cells previously treated with the dual NLRP1/NLRP3
595 inflammasome inhibitor ADS032 (100 µM, MedChemExpress) were included.

596 Flow cytometry

597 For studying the protein expression, before and after pro-inflammatory stimulation, NK cells were
598 stained with LIVE/DEAD AQUA viability (Invitrogen) for 20 minutes at room temperature (RT). After
599 washing once with staining buffer (1X PBS 3% FBS), cells were surface stained with anti-CD56-FITC
600 (B159, Becton Dickinson), and anti-CD3-PE-Cy7 (SK7, Becton Dickinson) antibodies for 20 mins at RT.
601 Next, we performed a washing step, and cells were fixed and permeabilized with
602 Fixation/Permeabilization Solution (Becton Dickinson) for 20 minutes at 4ºC and then washed with
603 BD Perm/Wash buffer. After, cells were stained with rabbit anti-NLRP1 (A16212 ABclonal) for 20
604 mins at RT, washed, and detected by staining with an anti-rabbit secondary AF750 (ab175735,
605 Abcam) antibody for an additional 20 mins at RT. Another washing step was performed and staining
606 with anti-NLRP3-AF700 (768319, R&D Systems) and anti-ASC-PE (HASC-71, Biolegend) was carried
607 out for 20 minutes at RT. Finally, cells were washed with BD Perm/Wash.

608 We also studied the expression of the inflammasome components in NK cells and monocytes from
609 kidney-injured patients, before and after being subjected to kidney transplantation. PBMCs from
610 these patients were stained with LIVE/DEAD AQUA viability (Invitrogen), and then, with anti-CD56-
611 FITC (B159, Becton Dickinson), anti-CD3-PE-Cy7 (SK7, Becton Dickinson), anti-CD4-BV605 (RPA-T4,
612 Becton Dickinson), anti-HLA-DR-PE-Da594 (L243, Biolegend), and anti-CD14-APC-H7 (M5E2, Becton
613 Dickinson) antibodies. Cells were subsequently fixed and permeabilized with
614 Fixation/Permeabilization Solution (Becton Dickinson) and intracellularly stained with anti-NLRP1-
615 AF647 (vwr), anti-NLRP3-AF700 (768319, R&D Systems) and anti-ASC-PE (HASC-71, Biolegend).
616 Samples were acquired on a CELESTA flow cytometer, and data was analyzed using FlowJo V10
617 software. Gating was performed according to the different FMO controls.

618 Western blot assays

619 Western blotting was performed using standard methods. Total PMBCs or NK cell extracted proteins
620 were used for standard protein electrophoresis and Western blot assays. Gel electrophoresis was
621 performed using 4–20% Mini-PROTEAN® TGX Stain-Free™ Protein Gels, Biorad at 200V in Tris-
622 Glycine-SDS buffer for 40 mins. Protein transfer was made using a TurboTransfer (Biorad, Hercules,
623 CA, USA) at 25V for 7 mins. After transferring the proteins to 0.45 µM nitrocellulose membranes
624 (Biorad, Hercules, CA, USA), these were incubated for 1 hour in BSA 5% in PBS-Tween20 0.05% and
625 then overnight at 4ºC with primary antibodies at 1:1,000 dilution. Then washed twice with PBS-
626 Tween20 and incubated with the corresponding secondary antibody coupled to horseradish

627 peroxidase diluted 1:10,000 for 1h at RT. Protein loading was checked using stain-free gel activation
628 and tubulin protein amount. Stripping was not used.

629 The following primary antibodies were used: NLRP1 (ABclonal, A16212), NLRP3 (ABclonal, A5652),
630 Caspase-1 (Cell signaling, 3866S), Gasdermin D (Santacruz, sc-393581), Caspase-4 (F4T9L) (Cell
631 signaling, 42264T), GADPH (Cell signaling, 5174S). Anti-rabbit or anti-mouse IgG secondary antibody
632 from Calbiochem was used.

633 Analysis of cytokine and immune factor secretion

634 Concentrations of the cytokines and molecules GM-CSF, IFN-γ, IL-1β, IL-6, IL-10, TNF-α, IL-18, IFN-α,
635 and ICAM-1 were quantified in 50 µL of supernatant from stimulated NK cells using a bead-based
636 multiplex immunoassay (ProcartaPlex; Invitrogen) according to the manufacturer's
637 recommendations. Measurements were performed using a Luminex Intelliflex instrument
638 (ThermoFisher Scientific) and analyzed using a standard curve for each cytokine.

639 LDH cytotoxicity assay

640 Cell death was measured by lactate dehydrogenase (LDH) release in the supernatant following the
641 manufacturer's instructions (abcam). In these experiments, cells were plated and stimulated in
642 RPMI 1640 without FBS to not interfere with the assay.

643 Fluorescent flow cytometry imaging for ASC specking analyses.

644 Isolated NK cells and monocytes stimulated with Nigericin (10 µM, 50 minutes) with and without
645 previous treatment with the NLRP1/NLRP3 dual inhibitor ADS032 (100 µM, 45 mins before adding
646 Nigericin) were stained in 100 µl of staining buffer (PBS 3% FBS) with CD14-PE-Cy7 (HCD14,
647 Biolegend), CD3-AF488 (SP34-2, BD), CD56-BV421 (NCAM16.2, BD). Cells were then washed and
648 fixed and permeabilized with Fixation/Permeabilization Solution (Becton Dickinson) for 20 minutes
649 at 4ºC. After a wash with BD Perm/Wash buffer, cells were intracellularly stained with ASC-PE (HASC-
650 71, Biolegend), and NLRP1-AF647 (vwr) or NLRP3-AF700 (768319, R&D Systems) antibodies. Cells
651 were acquired with an AMNIS ImageStreamX imaging flow cytometer (Merck), and data was
652 analyzed using IDEAS v6.1 software.

653 Quantification and statistical analysis

654 Statistical analyses were performed with Prism software, version 6.0 (GraphPad). A P value <0.05
655 was considered significant. The statistical details for the different experiments can be found in each
656 figure legend.

657

658

659

660

661

662

663

664

665

666

667

668

669

670

671

672

673

674

675

676 **REFERENCES**

677 1. Zitti, B. and Y.T. Bryceson, *Natural killer cells in inflammation and autoimmunity.* Cytokine
678 Growth Factor Rev, 2018. **42**: p. 37–46.
679 2. Horowitz, A., et al., *Genetic and environmental determinants of human NK cell diversity*
680 *revealed by mass cytometry.* Sci Transl Med, 2013. **5**(208): p. 208ra145.
681 3. Dogra, P., et al., *Tissue Determinants of Human NK Cell Development, Function, and*
682 *Residence.* Cell, 2020. **180**(4): p. 749–763 e13.
683 4. Moretta, L., *Dissecting CD56dim human NK cells.* Blood, 2010. **116**(19): p. 3689–91.
684 5. Vivier, E., et al., *Functions of natural killer cells.* Nat Immunol, 2008. **9**(5): p. 503–10.
685 6. Lanier, L.L., *Up on the tightrope: natural killer cell activation and inhibition.* Nat Immunol,
686 2008. **9**(5): p. 495–502.
687 7. Fauriat, C., et al., *Regulation of human NK-cell cytokine and chemokine production by target*
688 *cell recognition.* Blood, 2010. **115**(11): p. 2167–76.
689 8. Erlich, Z., et al., *Macrophages, rather than DCs, are responsible for inflammasome activity*
690 *in the GM-CSF BMDC model.* Nat Immunol, 2019. **20**(4): p. 397–406.
691 9. Migita, K., et al., *Serum amyloid A triggers the mosodium urate -mediated mature*
692 *interleukin-1beta production from human synovial fibroblasts.* Arthritis Res Ther, 2012.
693 **14**(3): p. R119.
694 10. Lei-Leston, A.C., A.G. Murphy, and K.J. Maloy, *Epithelial Cell Inflammasomes in Intestinal*
695 *Immunity and Inflammation.* Front Immunol, 2017. **8**: p. 1168.
696 11. Talley, S., D.J. Rademacher, and E.M. Campbell, *Inflammasome activation occurs in CD4(+)*
697 *and CD8(+) T cells during graft-versus-host disease.* Cell Death Dis, 2023. **14**(9): p. 632.
698 12. Zheng, D., T. Liwinski, and E. Elinav, *Inflammasome activation and regulation: toward a*
699 *better understanding of complex mechanisms.* Cell Discov, 2020. **6**: p. 36.
700 13. Swanson, K.V., M. Deng, and J.P. Ting, *The NLRP3 inflammasome: molecular activation and*
701 *regulation to therapeutics.* Nat Rev Immunol, 2019. **19**(8): p. 477–489.
702 14. Dai, Z., et al., *Gasdermin D-mediated pyroptosis: mechanisms, diseases, and inhibitors.* Front
703 Immunol, 2023. **14**: p. 1178662.
704 15. Martinon, F. and J. Tschopp, *Inflammatory caspases: linking an intracellular innate immune*
705 *system to autoinflammatory diseases.* Cell, 2004. **117**(5): p. 561–74.
706 16. Ghait, M., et al., *The non-canonical inflammasome activators Caspase-4 and Caspase-5 are*
707 *differentially regulated during immunosuppression-associated organ damage.* Front
708 Immunol, 2023. **14**: p. 1239474.
709 17. Wei, Y., et al., *Inflammation-Related Genes Serve as Prognostic Biomarkers and Involve in*
710 *Immunosuppressive Microenvironment to Promote Gastric Cancer Progression.* Front Med
711 (Lausanne), 2022. **9**: p. 801647.
712 18. Costa Franco, M.M., et al., *Brucella abortus Triggers a cGAS-Independent STING Pathway To*
713 *Induce Host Protection That Involves Guanylate-Binding Proteins and Inflammasome*
714 *Activation.* J Immunol, 2018. **200**(2): p. 607–622.
715 19. Gomes, M.T.R., et al., *Guanylate-binding proteins at the crossroad of noncanonical*
716 *inflammasome activation during bacterial infections.* J Leukoc Biol, 2019. **106**(3): p. 553–
717 562.
718 20. Zhong, F.L., et al., *Human DPP9 represses NLRP1 inflammasome and protects against*
719 *autoinflammatory diseases via both peptidase activity and FIIND domain binding.* J Biol
720 Chem, 2018. **293**(49): p. 18864–18878.
721 21. Okondo, M.C., et al., *DPP8 and DPP9 inhibition induces pro-caspase-1-dependent monocyte*
722 *and macrophage pyroptosis.* Nat Chem Biol, 2017. **13**(1): p. 46–53.

723 22. Sester, D.P., et al., *A novel flow cytometric method to assess inflammasome formation.* J
724 Immunol, 2015. **194**(1): p. 455–62.
725 23. Zheng, Z., et al., *NLRP3 associated with chronic kidney disease progression after*
726 *ischemia/reperfusion-induced acute kidney injury.* Cell Death Discov, 2021. **7**(1): p. 324.
727 24. Granata, S., et al., *NLRP3 inflammasome activation in dialyzed chronic kidney disease*
728 *patients.* PLoS One, 2015. **10**(3): p. e0122272.
729 25. Franchon Marques Tejada, N., et al., *AIM2 as a putative target in acute kidney graft*
730 *rejection.* Frontiers in Immunology, 2022. **13**.
731 26. Dessing, M.C., et al., *Donor and recipient genetic variants in NLRP3 associate with early*
732 *acute rejection following kidney transplantation.* Sci Rep, 2016. **6**: p. 36315.
733 27. Suarez-Rivero, J.M., et al., *Does NLRP1 inflammasome activation in immune cells in kidney*
734 *transplantation relate with donor organ age?* Antioxid Redox Signal, 2024.
735 28. Bohmig, G.A., et al., *Microvascular inflammation in kidney allografts: New directions for*
736 *patient management.* Am J Transplant, 2025. **25**(7): p. 1410–1416.
737 29. Yazdani, S., et al., *Natural killer cell infiltration is discriminative for antibody-mediated*
738 *rejection and predicts outcome after kidney transplantation.* Kidney Int, 2019. **95**(1): p. 188–
739 198.
740 30. Lamarthee, B., et al., *Transcriptional and spatial profiling of the kidney allograft unravels a*
741 *central role for FcyRIII+ innate immune cells in rejection.* Nat Commun, 2023. **14**(1): p. 4359.
742 31. Diebold, M., et al., *Natural Killer Cell Presence in Antibody-Mediated Rejection.* Transpl Int,
743 2024. **37**: p. 13209.
744 32. Van Loon, E., et al., *Biological pathways and comparison with biopsy signals and cellular*
745 *origin of peripheral blood transcriptomic profiles during kidney allograft pathology.* Kidney
746 International, 2022. **102**(1): p. 183–195.
747 33. Shi, J., et al., *Cleavage of GSDMD by inflammatory caspases determines pyroptotic cell*
748 *death.* Nature, 2015. **526**(7575): p. 660–5.
749 34. Qiu, F., et al., *Activation of cytokine-producing and antitumor activities of natural killer cells*
750 *and macrophages by engagement of Toll-like and NOD-like receptors.* Innate Immun, 2011.
751 **17**(4): p. 375–87.
752 35. Broz, P. and V.M. Dixit, *Inflammasomes: mechanism of assembly, regulation and signalling.*
753 Nat Rev Immunol, 2016. **16**(7): p. 407–20.
754 36. Rozario, P., et al., *Mechanistic basis for potassium efflux-driven activation of the human*
755 *NLRP1 inflammasome.* Proc Natl Acad Sci U S A, 2024. **121**(2): p. e2309579121.
756 37. Henderson, P.J., *Ion transport by energy-conserving biological membranes.* Annu Rev
757 Microbiol, 1971. **25**: p. 393–428.
758 38. Taabazuing, C.Y., A.R. Griswold, and D.A. Bachovchin, *The NLRP1 and CARD8*
759 *inflammasomes.* Immunol Rev, 2020. **297**(1): p. 13–25.
760 39. Volchuk, A., et al., *Indirect regulation of HMGB1 release by gasdermin D.* Nat Commun,
761 2020. **11**(1): p. 4561.
762 40. Michel, T., et al., *Human CD56bright NK Cells: An Update.* J Immunol, 2016. **196**(7): p. 2923–
763 31.
764 41. Osuka, A., et al., *A protective role for inflammasome activation following injury.* Shock, 2012.
765 **37**(1): p. 47–55.
766 42. Stoecklein, V.M., et al., *Radiation exposure induces inflammasome pathway activation in*
767 *immune cells.* J Immunol, 2015. **194**(3): p. 1178–89.
768 43. Fong, J.J., et al., *Siglec-7 engagement by GBS beta-protein suppresses pyroptotic cell death*
769 *of natural killer cells.* Proc Natl Acad Sci U S A, 2018. **115**(41): p. 10410–10415.

770 44. Souza-Fonseca-Guimaraes, F., et al., *Toll-like receptors expression and interferon-gamma*
771 *production by NK cells in human sepsis.* Crit Care, 2012. **16**(5): p. R206.
772 45. Zhu, L., et al., *Changes of NK cell subsets with time post-transplant in peripheral blood of*
773 *renal transplant recipients.* Transpl Immunol, 2018. **49**: p. 59–71.
774 46. Pontrelli, P., et al., *The Role of Natural Killer Cells in the Immune Response in Kidney*
775 *Transplantation.* Front Immunol, 2020. **11**: p. 1454.
776 47. Venner, J.M., et al., *The molecular landscape of antibody-mediated kidney transplant*
777 *rejection: evidence for NK involvement through CD16a Fc receptors.* Am J Transplant, 2015.
778 **15**(5): p. 1336–48.
779 48. Callemeyn, J., et al., *Allorecognition and the spectrum of kidney transplant rejection.* Kidney
780 Int, 2022. **101**(4): p. 692–710.
781 49. Sablik, M., et al., *Microvascular Inflammation of Kidney Allografts and Clinical Outcomes.* N
782 Engl J Med, 2025. **392**(8): p. 763–776.
783 50. Halloran, P.F., et al., *Molecular diagnosis of ABMR with or without donor-specific antibody*
784 *in kidney transplant biopsies: Differences in timing and intensity but similar mechanisms and*
785 *outcomes.* Am J Transplant, 2022. **22**(8): p. 1976–1991.
786 51. Callemeyn, J., et al., *Missing Self-Induced Microvascular Rejection of Kidney Allografts: A*
787 *Population-Based Study.* J Am Soc Nephrol, 2021. **32**(8): p. 2070–2082.
788 52. Mayer, K.A., et al., *A Randomized Phase 2 Trial of Felzartamab in Antibody-Mediated*
789 *Rejection.* N Engl J Med, 2024. **391**(2): p. 122–132.
790 53. Diebold, M., et al., *Effect of felzartamab on the molecular phenotype of antibody-mediated*
791 *rejection in kidney transplant biopsies.* Nat Med, 2025. **31**(5): p. 1668–1676.
792 54. Shua, Y., et al., *Progress in small-molecule inhibitors of gasdermin D.* European Journal of
793 Medicinal Chemistry, 2025. **300**: p. 118171.
794 55. Docherty, C.A., et al., *A novel dual NLRP1 and NLRP3 inflammasome inhibitor for the*
795 *treatment of inflammatory diseases.* Clin Transl Immunology, 2023. **12**(6): p. e1455.

796

Figure 1

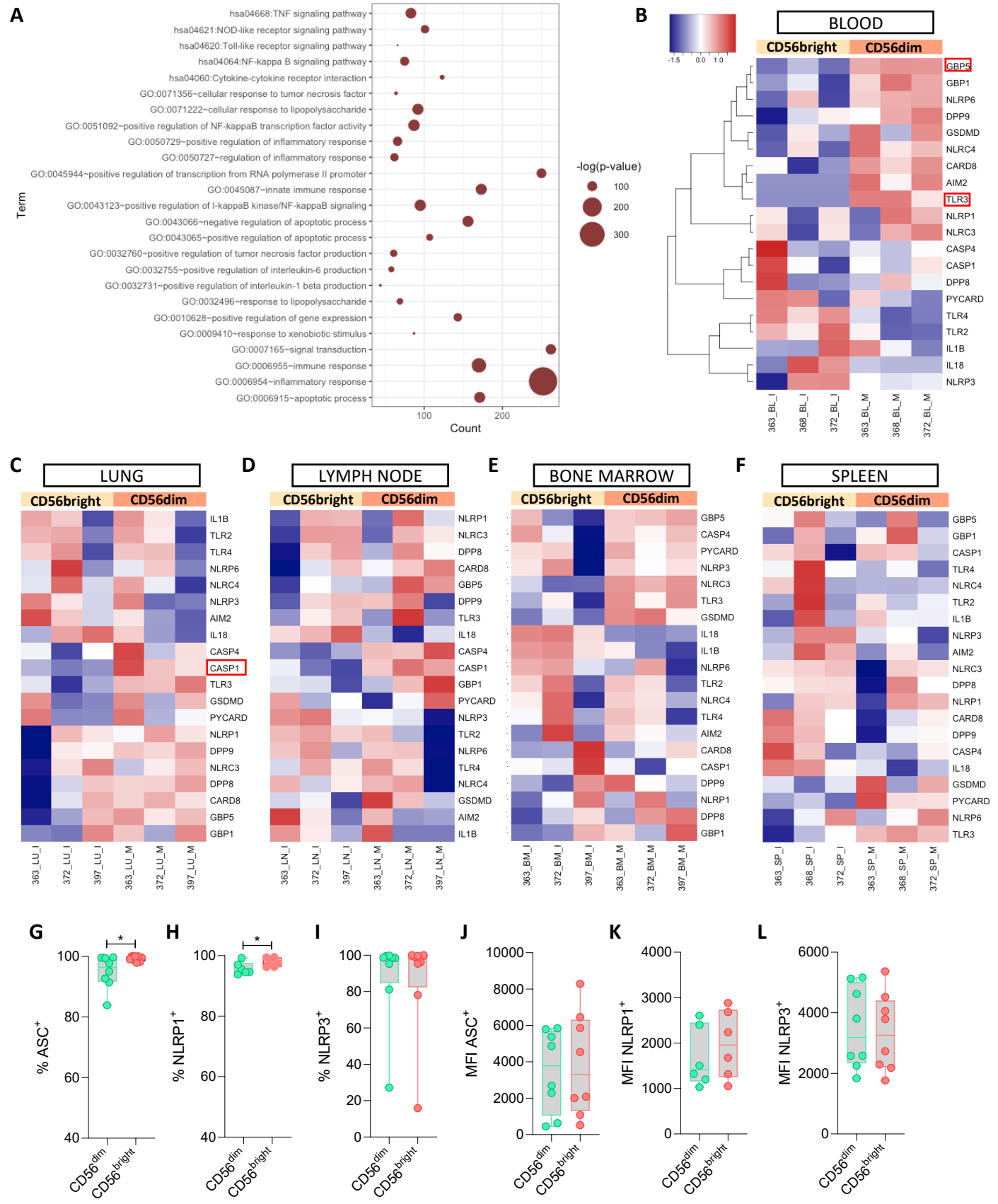
A
hsa04668:TNF signaling pathway
hsa04621:NOD-like receptor signaling pathway
hsa04620:Toll-like receptor signaling pathway
hsa04064:NF-kappa B signaling pathway
hsa04060:Cytokine-cytokine receptor interaction
GO:0071356~cellular response to tumor necrosis factor
GO:0071222~cellular response to lipopolysaccharide
GO:0051092~positive regulation of NF-kappaB transcription factor activity
GO:0050729~positive regulation of inflammatory response
GO:0050727~regulation of inflammatory response
GO:0045944~positive regulation of transcription from RNA polymerase II promoter
GO:0045087~innate immune response
GO:0043123~positive regulation of I-kappaB kinase/NF-kappaB signaling
GO:0043066~negative regulation of apoptotic process
GO:0043065~positive regulation of apoptotic process
GO:0032760~positive regulation of tumor necrosis factor production
GO:0032755~positive regulation of interleukin-6 production
GO:0032731~positive regulation of interleukin-1 beta production
GO:0032496~response to lipopolysaccharide
GO:0010628~positive regulation of gene expression
GO:0009410~response to xenobiotic stimulus
GO:0007165~signal transduction
GO:0006955~immune response
GO:0006954~inflammatory response
GO:0006915~apoptotic process
Term
Count
100
200
-log(p-value)
100
200
300
B
BLOOD
CD56bright
CD56dim
-1.5
0.0
1.0
GBP5
GBP1
NLRP6
DPP9
GSDMD
NLRC4
CARD8
AIM2
TLR3
NLRP1
NLRC3
CASP4
CASP1
DPP8
PYCARD
TLR4
TLR2
IL1B
IL18
NLRP3
363_BL_I
368_BL_I
372_BL_I
363_BL_M
368_BL_M
372_BL_M
C
LUNG
CD56bright
CD56dim
IL1B
TLR2
TLR4
NLRP6
NLRC4
NLRP3
AIM2
IL18
CASP4
CASP1
TLR3
GSDMD
PYCARD
NLRP1
DPP9
NLRC3
DPP8
CARD8
GBP5
GBP1
363_LU_I
372_LU_I
397_LU_I
363_LU_M
372_LU_M
397_LU_M
D
LYMPH NODE
CD56bright
CD56dim
NLRP1
NLRC3
DPP8
CARD8
GBP5
DPP9
TLR3
IL18
CASP4
CASP1
GBP1
PYCARD
NLRP3
TLR2
NLRP6
TLR4
NLRC4
GSDMD
AIM2
IL1B
363_LN_I
372_LN_I
397_LN_I
363_LN_M
372_LN_M
397_LN_M
E
BONE MARROW
CD56bright
CD56dim
GBP5
CASP4
PYCARD
NLRP3
NLRC3
TLR3
GSDMD
IL18
IL1B
NLRP6
TLR2
NLRC4
TLR4
AIM2
CARD8
CASP1
DPP9
NLRP1
DPP8
GBP1
363_BM_I
372_BM_I
397_BM_I
363_BM_M
372_BM_M
397_BM_M
F
SPLEEN
CD56bright
CD56dim
GBP5
GBP1
CASP1
TLR4
NLRC4
TLR2
IL1B
NLRP3
AIM2
NLRC3
DPP8
NLRP1
CARD8
DPP9
CASP4
IL18
GSDMD
PYCARD
NLRP6
TLR3
363_SP_I
368_SP_I
372_SP_I
363_SP_M
368_SP_M
372_SP_M
G
% ASC+
100
80
60
40
*
CD56dim
CD56bright
H
% NLRP1+
100
80
60
40
*
CD56dim
CD56bright
I
% NLRP3+
100
80
60
40
20
0
CD56dim
CD56bright
J
MFI ASC+
10000
8000
6000
4000
2000
0
CD56dim
CD56bright
K
MFI NLRP1+
4000
3000
2000
1000
0
CD56dim
CD56bright
L
MFI NLRP3+
6000
4000
2000
0
CD56dim
CD56bright

Figure 2

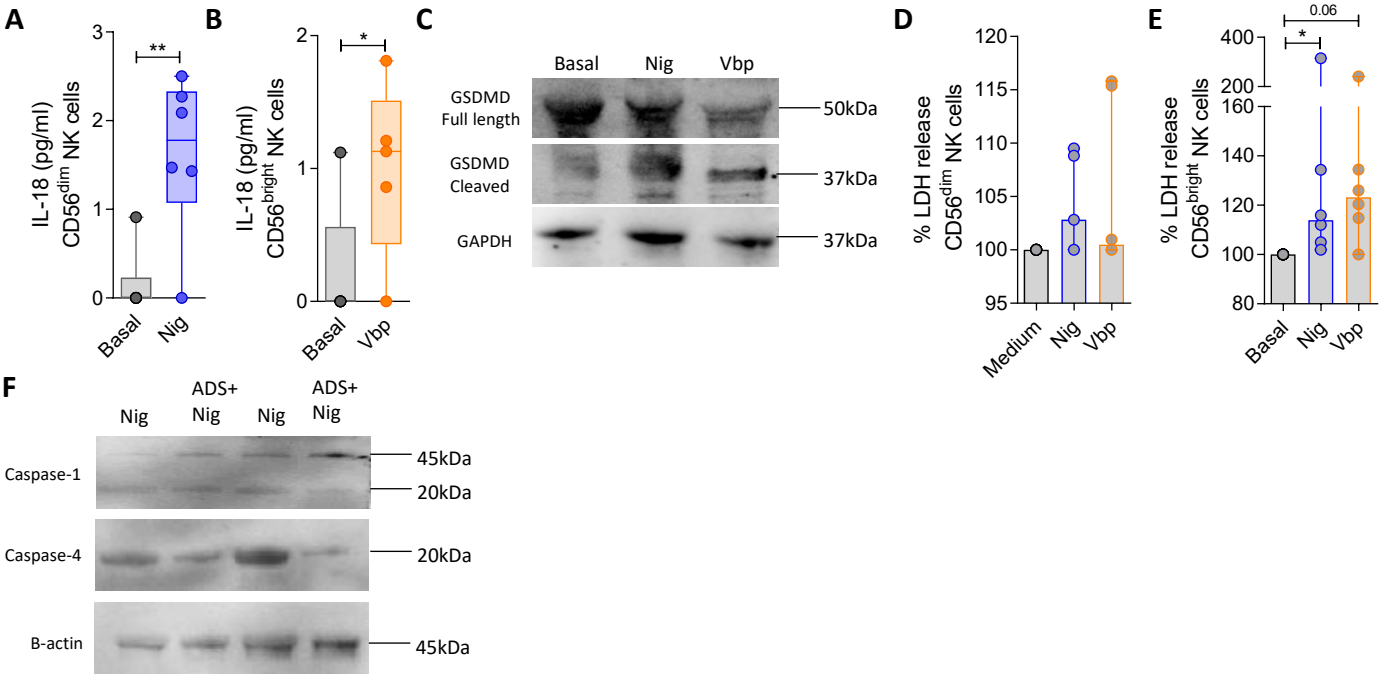
A
IL-18 (pg/ml) CD56dim NK cells
**
Basal
Nig
B
IL-18 (pg/ml) CD56bright NK cells
*
Basal
Vbp
C
Basal
Nig
Vbp
GSDMD Full length
GSDMD Cleaved
GAPDH
50kDa
37kDa
37kDa
D
% LDH release CD56dim NK cells
Medium
Nig
Vbp
E
% LDH release CD56bright NK cells
0.06
*
Basal
Nig
Vbp
F
Nig
ADS+ Nig
Nig
ADS+ Nig
Caspase-1
Caspase-4
B-actin
45kDa
20kDa
20kDa
45kDa

Figure 3

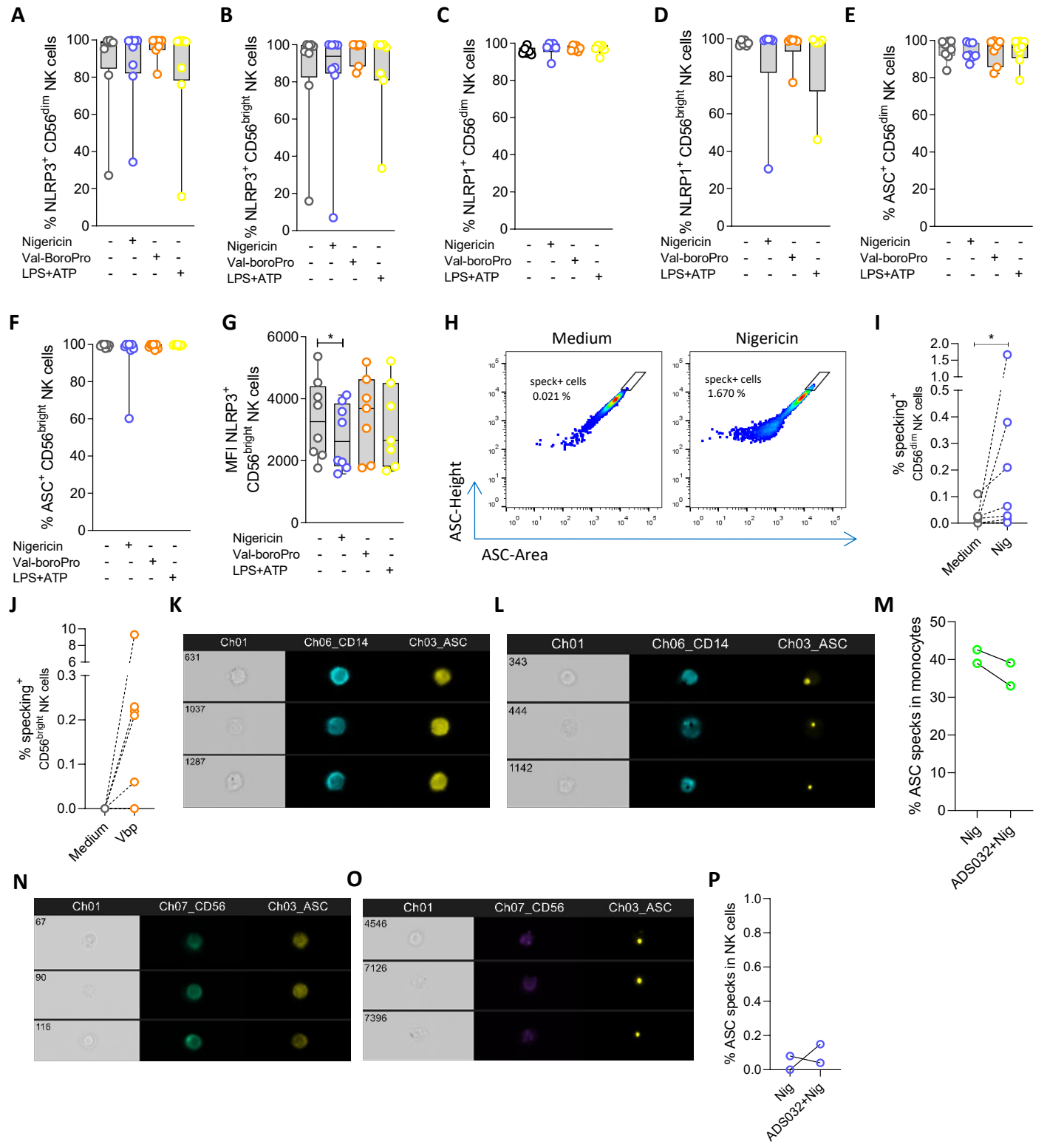
A
% NLRP3+ CD56dim NK cells
B
% NLRP3+ CD56bright NK cells
C
% NLRP1+ CD56dim NK cells
D
% NLRP1+ CD56bright NK cells
E
% ASC+ CD56dim NK cells
F
% ASC+ CD56bright NK cells
G
MFI NLRP3+ CD56bright NK cells
Nigericin
Val-boroPro
LPS+ATP
H
Medium
Nigericin
speck+ cells 0.021 %
speck+ cells 1.670 %
ASC-Height
ASC-Area
I
% specking+ CD56dim NK cells
Medium
Nig
J
% specking+ CD56bright NK cells
Medium
Vbp
K
Ch01
Ch06_CD14
Ch03_ASC
L
M
% ASC specks in monocytes
Nig
ADS032+Nig
N
Ch07_CD56
O
P
% ASC specks in NK cells

Figure 4

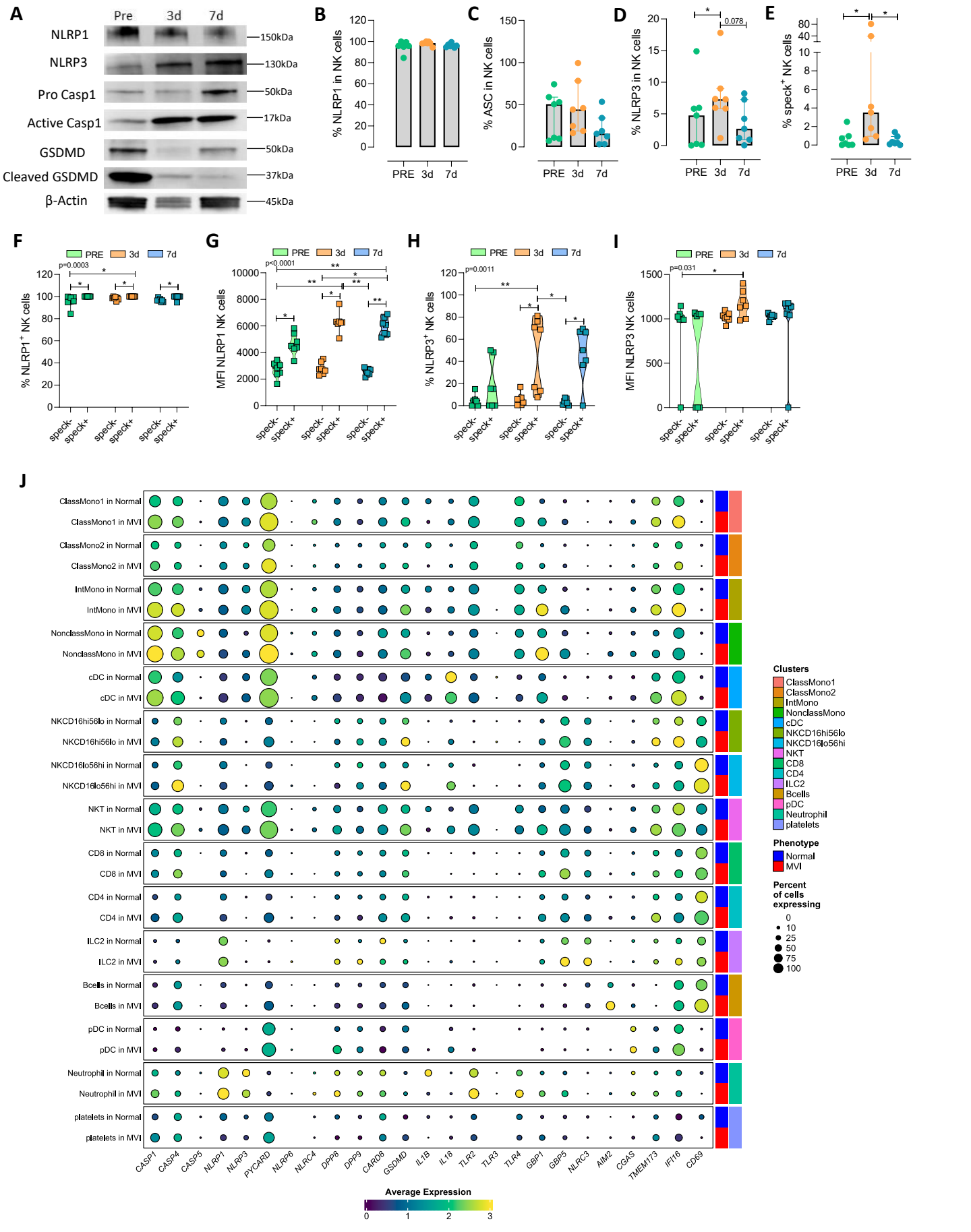
A
Pre
3d
7d
NLRP1
NLRP3
Pro Casp1
Active Casp1
GSDMD
Cleaved GSDMD
β-Actin
150kDa
130kDa
50kDa
17kDa
50kDa
37kDa
45kDa
B
% NLRP1 in NK cells
C
% ASC in NK cells
D
% NLRP3 in NK cells
0.078
E
% speck+ NK cells
PRE 3d 7d
F
% NLRP1+ NK cells
p=0.0003
G
MFI NLRP1 NK cells
p<0.0001
H
% NLRP3+ NK cells
p=0.0011
I
MFI NLRP3 NK cells
p=0.031
PRE 3d 7d
speck- speck+
J
ClassMono1 in Normal
ClassMono1 in MVI
ClassMono2 in Normal
ClassMono2 in MVI
IntMono in Normal
IntMono in MVI
NonclassMono in Normal
NonclassMono in MVI
cDC in Normal
cDC in MVI
NKCD16hi56lo in Normal
NKCD16hi56lo in MVI
NKCD16lo56hi in Normal
NKCD16lo56hi in MVI
NKT in Normal
NKT in MVI
CD8 in Normal
CD8 in MVI
CD4 in Normal
CD4 in MVI
ILC2 in Normal
ILC2 in MVI
Bcells in Normal
Bcells in MVI
pDC in Normal
pDC in MVI
Neutrophil in Normal
Neutrophil in MVI
platelets in Normal
platelets in MVI
CASP1 CASP4 CASP5 NLRP1 NLRP3 PYCARD NLRP6 NLRC4 DPP8 DPP9 CARD8 GSDMD IL1B IL18 TLR2 TLR3 TLR4 GBP1 GBP5 NLRC3 AIM2 CGAS TMEM173 IFI16 CD69
Clusters
ClassMono1
ClassMono2
IntMono
NonclassMono
cDC
NKCD16hi56lo
NKCD16lo56hi
NKT
CD8
CD4
ILC2
Bcells
pDC
Neutrophil
platelets
Phenotype
Normal
MVI
Percent of cells expressing
0
10
25
50
75
100
Average Expression
0 1 2 3

Figure 5

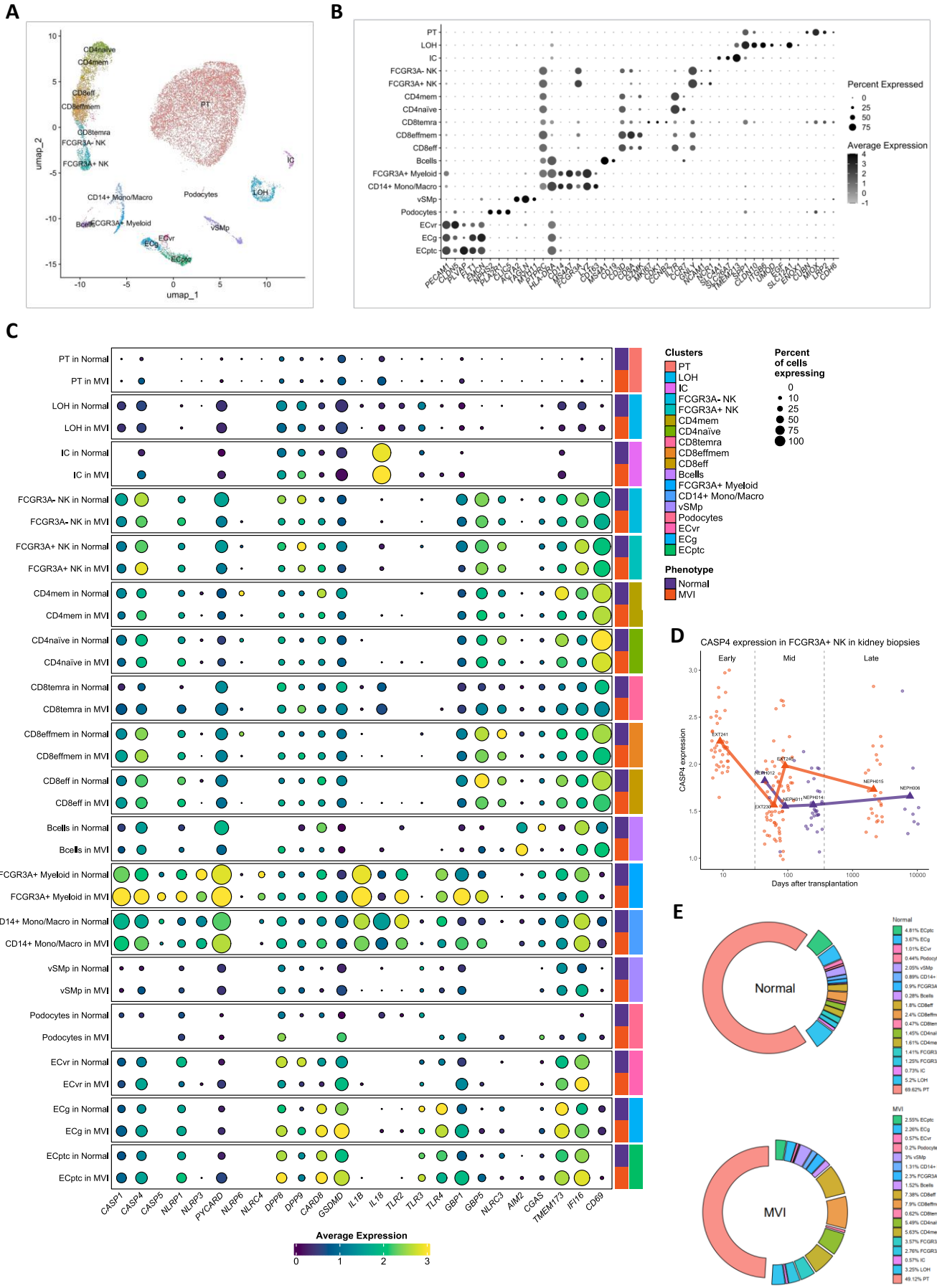
A
B
C
D
E
umap_1
umap_2
CD4naive
CD4mem
CD8eff
CD8effmem
CD8temra
FCGR3A- NK
FCGR3A+ NK
PT
IC
LOH
CD14+ Mono/Macro
Podocytes
Bcells
FCGR3A+ Myeloid
vSMp
ECvr
ECg
ECptc
Percent Expressed
Average Expression
Clusters
Percent of cells expressing
Phenotype
Normal
MVI
Average Expression
CASP4 expression in FCGR3A+ NK in kidney biopsies
Early
Mid
Late
CASP4 expression
Days after transplantation
Phenotype
MVI
Normal

Supplementary Figure 1

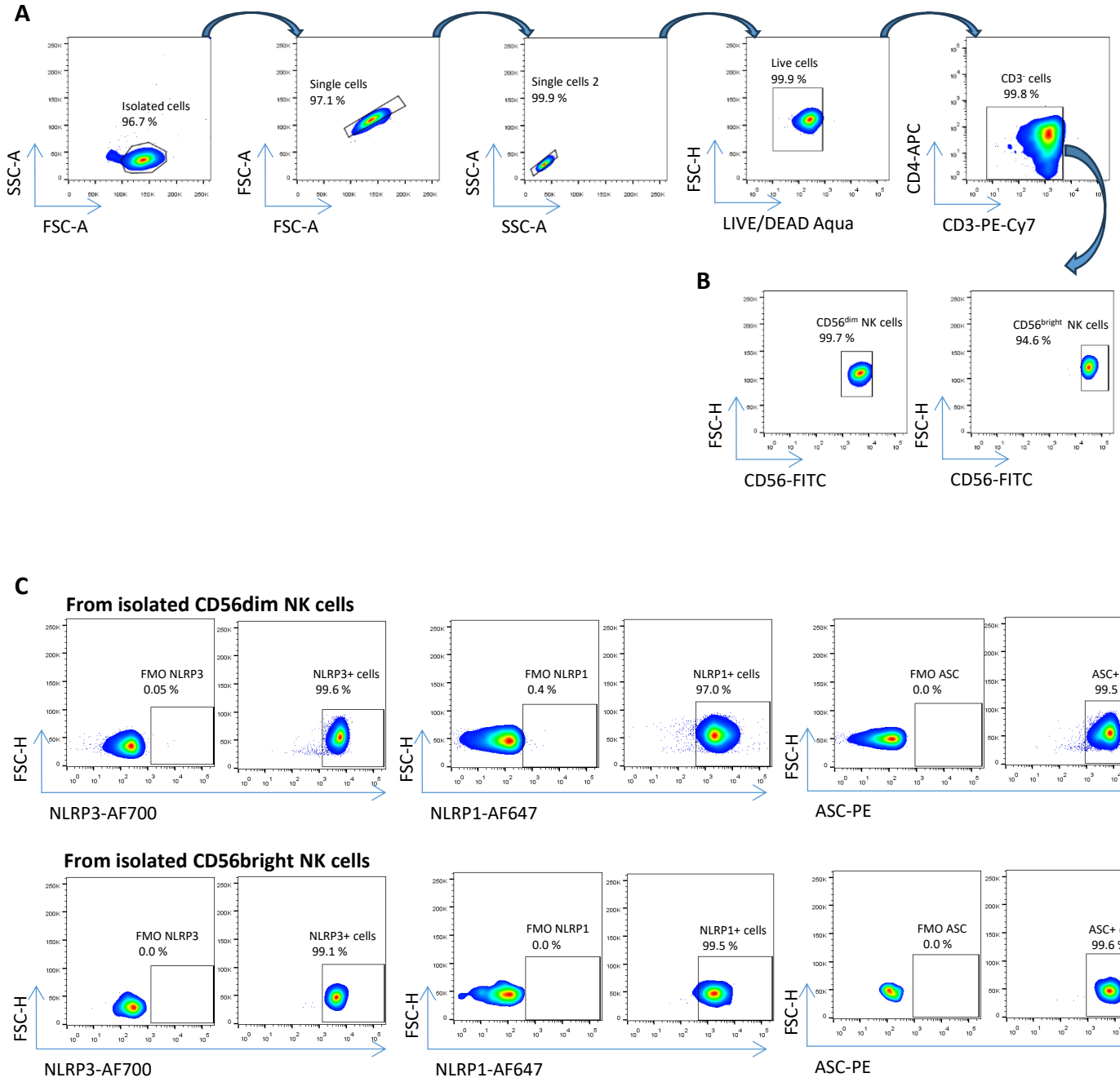

Supplementary Figure 2

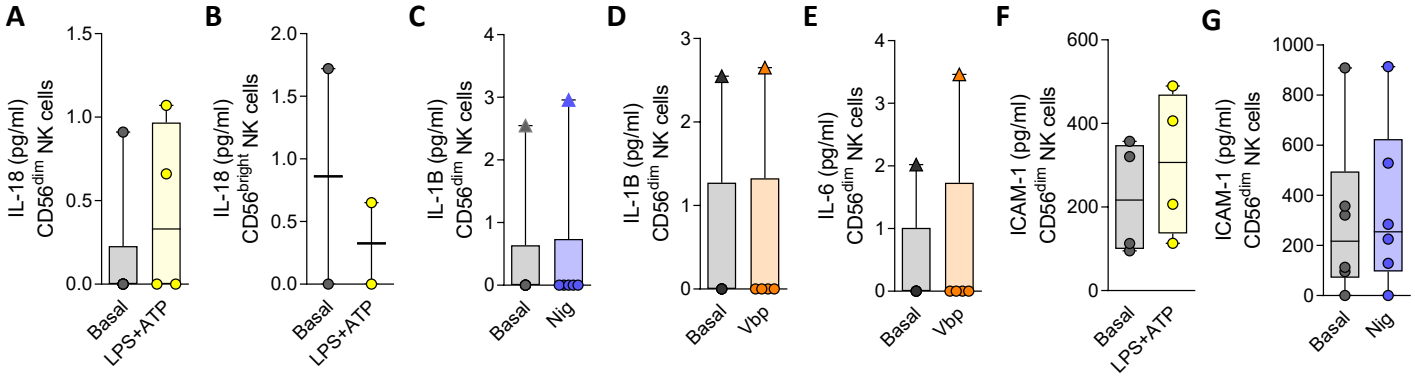

Supplementary Figure 3

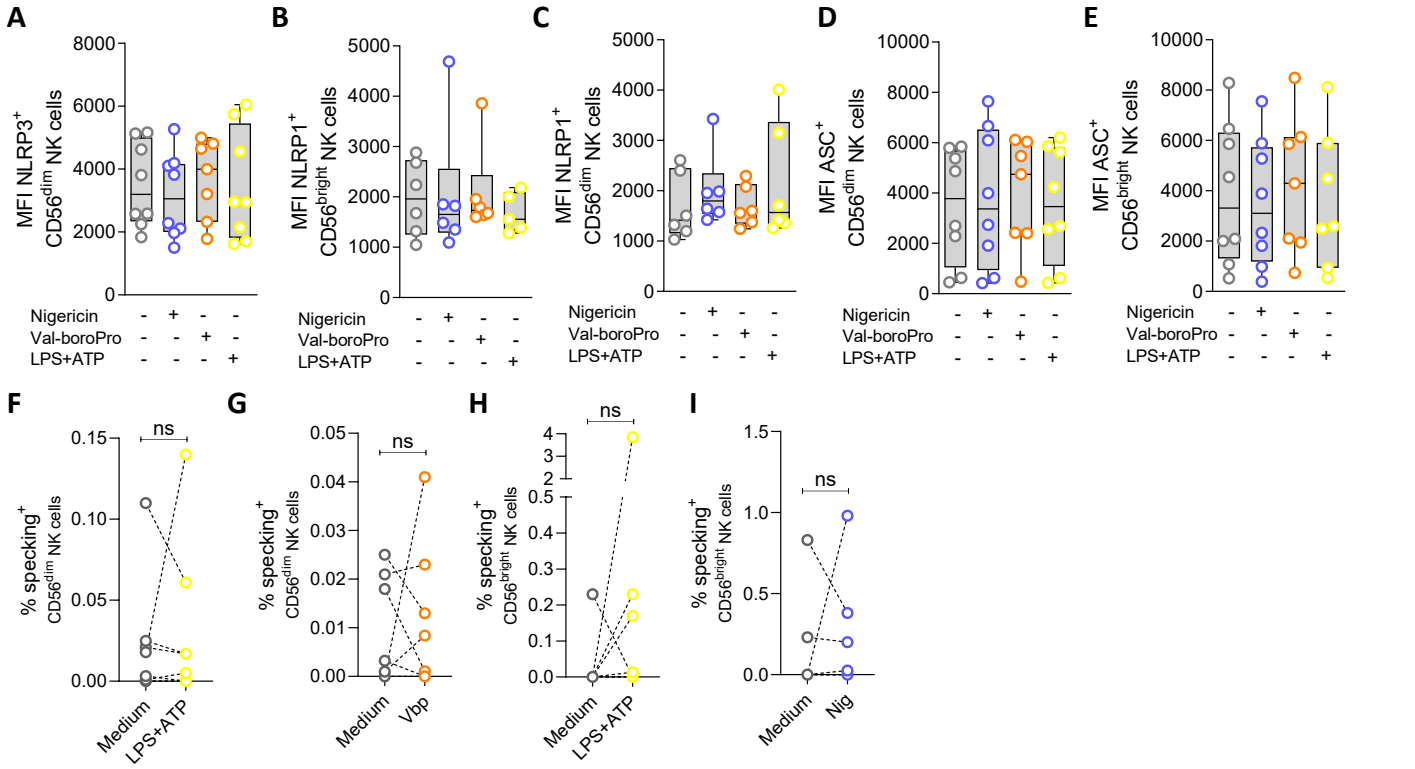

Supplementary Figure 4

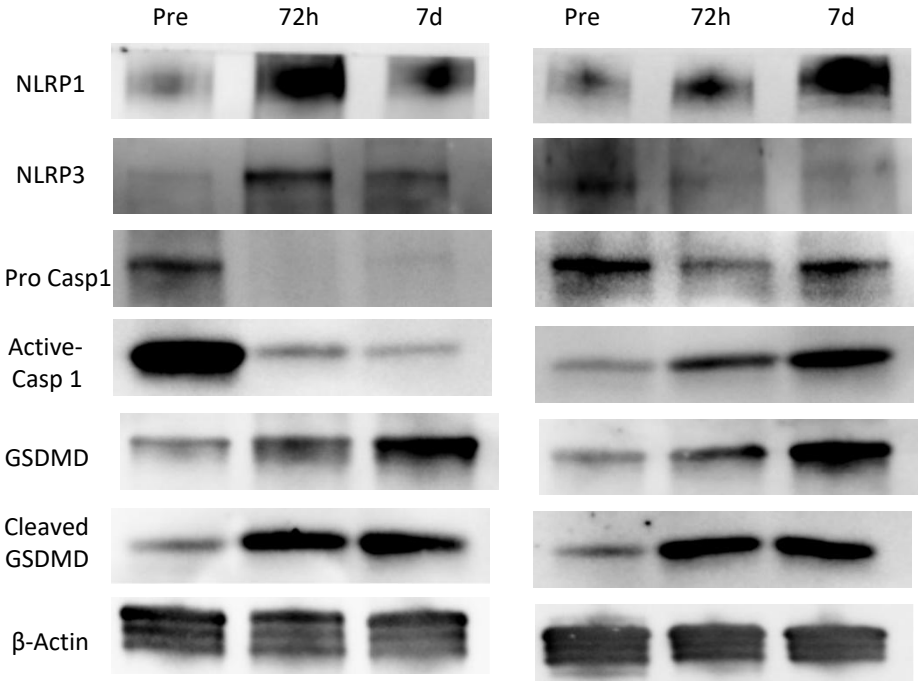

Supplementary Figure 5

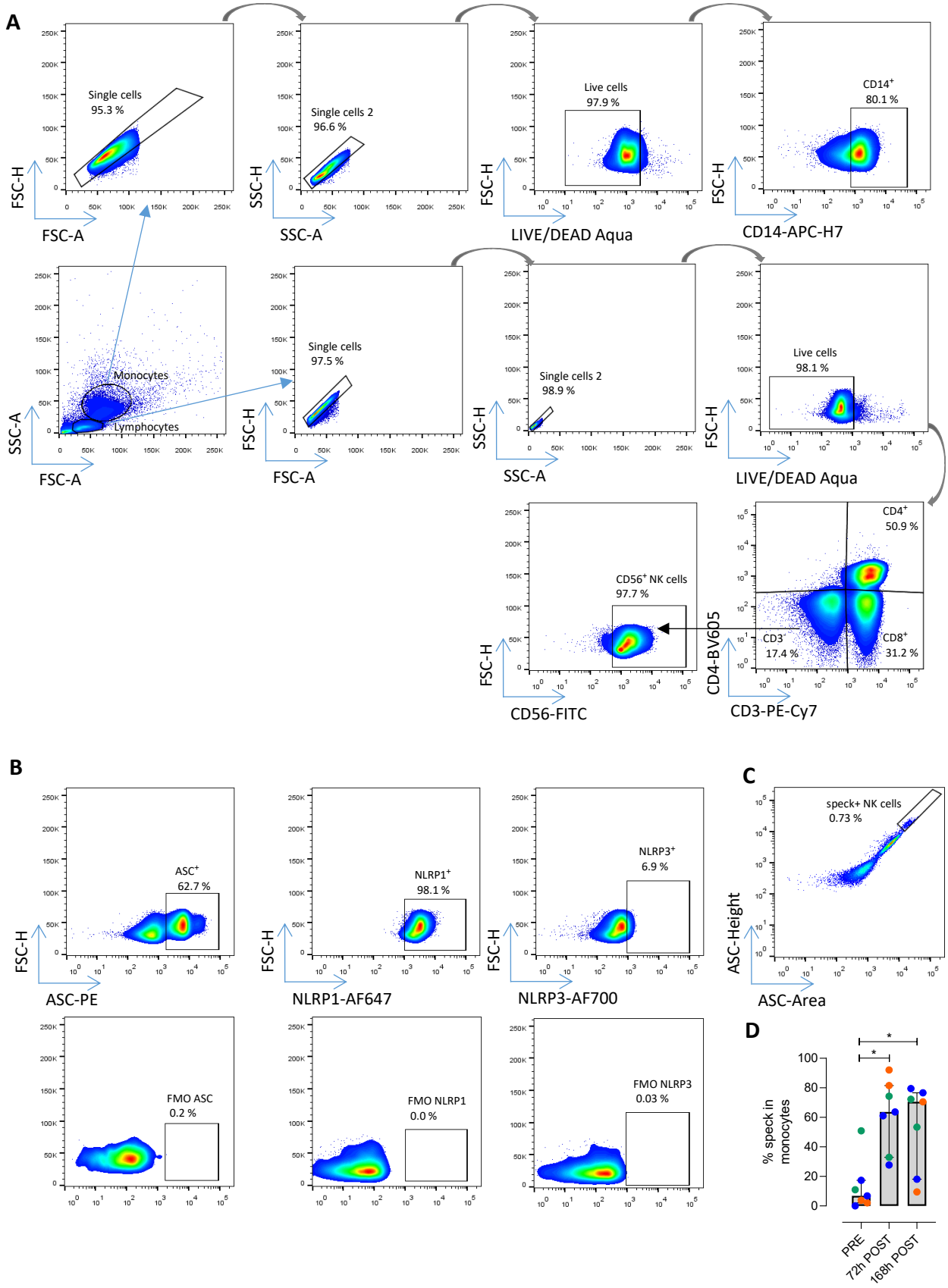

Supplementary Figure 6

A

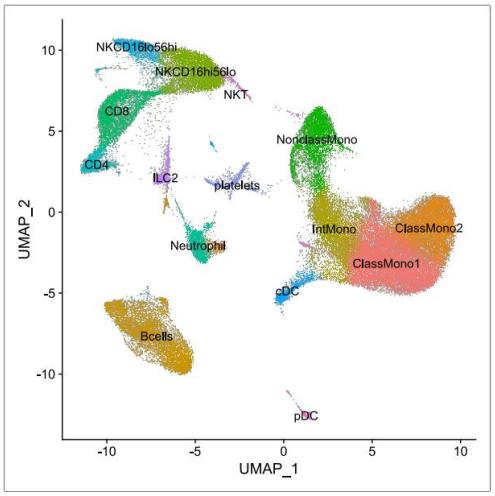

B

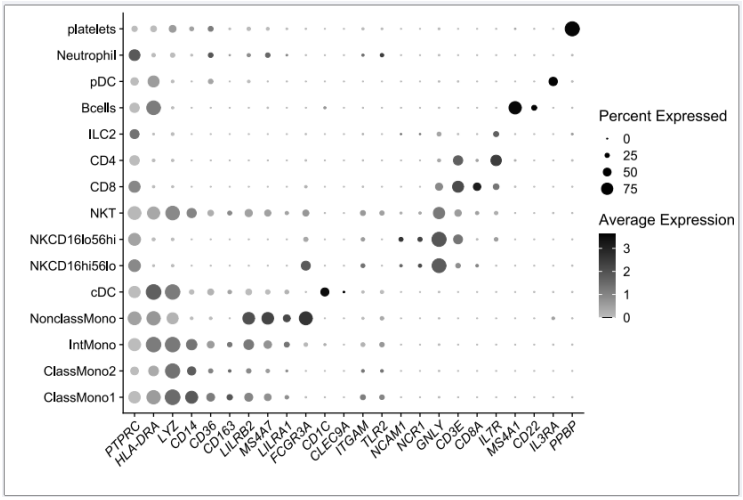

Supplementary Figure 7

A

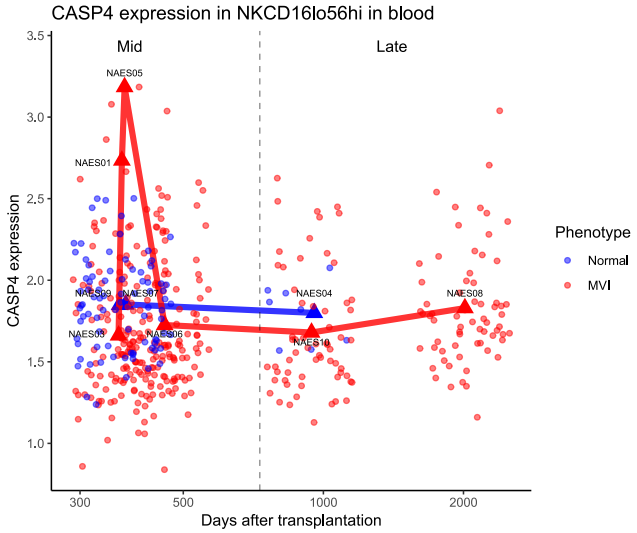
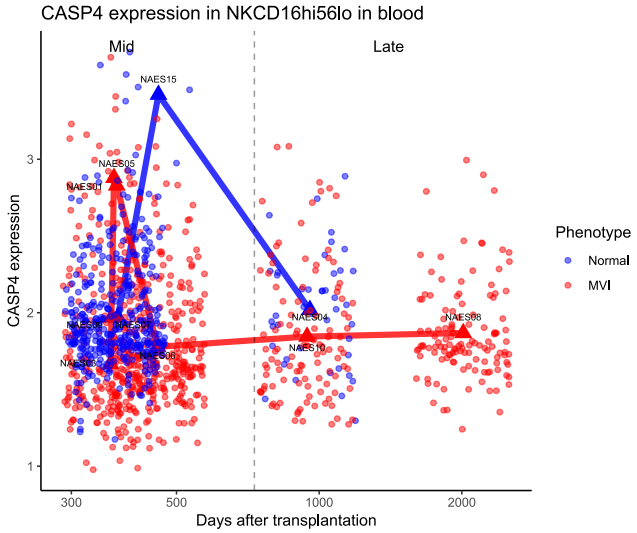
B